AD-A107 363 CARNEGIE-MELLON UNIV PITTSBURGH PA DEPT OF MECHANICA--ETC F/G 20/13
BOILING HEAT TRANSFER IN CONFINED SPACE.(U)
OCT 81 S YAO
UNCLASSIFIED N00014-79-C-0623
NL

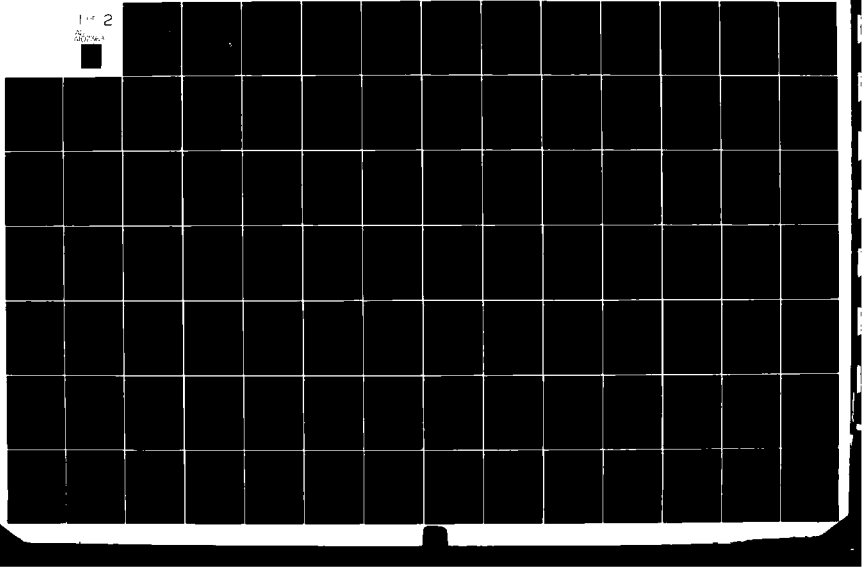

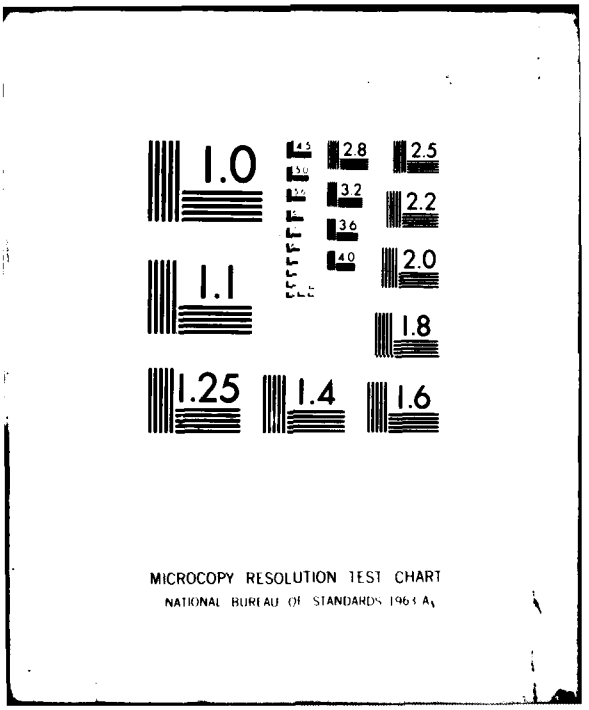
1.0
1.1
1.25
1.4
1.6
1.8
2.0
2.2
2.5
2.8
3.2
3.6
4.0
MICROCOPY RESOLUTION TEST CHART
NATIONAL BUREAU OF STANDARDS 1963 A

CMU Report N00014-79-C-0623-1981A

LEVEL II

12

Boiling Heat Transfer in Confined Space

Annual Technical Report
October 1981

S.C. Yao
Associate Professor
Department of Mechanical Engineering
Carnegie-Mellon University
Pittsburgh, PA 15213

Prepared for
M.K. Ellingsworth, Program Monitor
The Office of Naval Research
Arlington, VA 22217

Under Contract No. N00014-79-C-0623, Work Unit 097-436

102

UNCLASSIFIED

SECURITY CLASSIFICATION OF THIS PAGE (When Data Entered)

REPORT DOCUMENTATION PAGE

READ INSTRUCTIONS BEFORE COMPLETING FORM

1. REPORT NUMBER: N00014-79-C-0623-1981A	2. GOVT ACCESSION NO.: AD-A107363
3. RECIPIENT'S CATALOG NUMBER:	
4. TITLE (and Subtitle): BOILING HEAT TRANSFER IN CONFINED SPACE.	5. TYPE OF REPORT & PERIOD COVERED: Annual Technical Report. Aug. 1980 to Aug 1981
	6. PERFORMING ORG. REPORT NUMBER:
7. AUTHOR(s): Shi-chune Yao	8. CONTRACT OR GRANT NUMBER(s): N00014-79-C-0623
9. PERFORMING ORGANIZATION NAME AND ADDRESS: Dept. of Mechanical Engineering, Carnegie-Mellon University, Pittsburgh, PA 15213	10. PROGRAM ELEMENT, PROJECT, TASK AREA & WORK UNIT NUMBERS: Program Element 6115-3N, Project RRD2403, Task Area RR0240302, Work Unit NR097-436
11. CONTROLLING OFFICE NAME AND ADDRESS: Office of Naval Research, 800 N. Quincy Street, Arlington, VA 22217	12. REPORT DATE: October 1981
	13. NUMBER OF PAGES: 100
14. MONITORING AGENCY NAME & ADDRESS(if different from Controlling Office)	15. SECURITY CLASS. (of this report)
	15a. DECLASSIFICATION/DOWNGRADING SCHEDULE: Unclassified

16. DISTRIBUTION STATEMENT (of this Report)

Approved for public release; distribution unlimited.

DTIC ELECTE NOV 1 0 1981 D H

17. DISTRIBUTION STATEMENT (of the abstract entered in Block 20, if different from Report)

Same as Block No.16.

18. SUPPLEMENTARY NOTES

19. KEY WORDS (Continue on reverse side if necessary and identify by block number)

Boiling Heat Transfer, Dryout, Corrosion

20. ABSTRACT (Continue on reverse side if necessary and identify by block number)

In many equipments, boiling occurs in confined space such as the clearance between the tube and the support plate of steam generators. Corrosive concentration builds up at the boundary of dryout zone and induces severe damage. The knowledge on this kind of boiling phenomena is very limited. It is the objective of this research to understand this fundamental heat transfer of this problem through systematical analysis and experimental studies. —>

DD FORM 1 JAN 73 1473 EDITION OF 1 NOV 65 IS OBSOLETE S/N 0102-LF-014-6601

UNCLASSIFIED 405494

SECURITY CLASSIFICATION OF THIS PAGE (When Data Entered)

This report covers the following aspects of the boiling in confined space;(1) Analysis of single phase forced convection in support plate crevices;(2) Analysis of convective boiling and dryout in support plate crevices;(3) Experiments of boiling and dryout in annular crevices with closed bottom;and (4) Experiments of convective boiling and dryout in annular crevices.

CMU Report
N00014-79-C-0623-1981A

BOILING HEAT TRANSFER IN CONFINED SPACE

Annual Technical Report

October 1981

S.C. Yao
Associate Professor
Department of Mechanical Engineering
Carnegie-Mellon University
Pittsburgh, PA 15213

Prepared for

M.K. Ellingsworth, Program Monitor
The Office of Naval Research
Arlington, VA 22217

Under Contract No. N00014-79-C-0623, Work Unit 097-436

TABLE OF CONTENTS

SUMMARY

In many equipments, boiling occurs in confined space such as the clearance between the tube and the support plate of steam generators. Corrosive concentration builds up at the boundary of dryout zone and induces severe damage. The knowledge on this kind of boiling phenomena is very limited. It is the objective of this research to understand this fundamental heat transfer of this problem through systematical analysis and experimental studies.

This report describes the progress of research in the past year on the following areas:

Chapter 2. Analysis of single phase forced convection in the heat exchanger crevices between the tube and baffle-plate using creeping flow approximation for concentric, eccentric, and inclined annular geometries.

Chapter 3. Analysis of convective boiling and dryout in the support-plate crevices in steam generators. Compared with experimental data, and recommended for designs to avoid the dryout.

Chapter 4. Experiment of boiling and dryout in crevices with closed bottom for the application of tube-sheet crevices. Boiling in confined space is studied in detail with various fluids. The dryout in confined space is also studied for various geometry and fluids. A semi-empirical correlation is established.

Chapter 5. The current status of forced convective boiling and dryout in crevices is presented. The obtained data are discussed.

CONCLUSION

The fluid flow and heat transfer of the leakage stream between tube and baffle-plate in heat exchangers are studied for various possible geometries as indicated in Chapter 2. The information would be helpful for better design and performance evaluation of heat exchangers in general.

The boiling and dryout in support plate crevices can be calculated easily following the computation scheme stated in Chapter 3. The computation has been checked with experimental data. Better design and performance evaluation through computation becomes possible. To avoid dryout completely, square hole or holes with large difference in curvatures at contact point are recommended.

The boiling in confined space with closed bottom generally has high heat transfer coefficient but low critical heat flux. The Bond number is important in characterizing the boiling regimes. At critical heat flux, the mechanism is controlled by counterflow flooding. A correlation for various geometry and fluids is proposed. In general, it is independent of Bond number as inferred by the flooding correlation. Based upon this general correlation, the dryout of steam generator crevices in the tube-sheet can be estimated.

The convective boiling heat transfer in confined space has been reported here. It is similar to conventional boiling; however, the heat transfer coefficient is high and the critical heat flux is low. Further study are underway.

PUBLICATION OF THE PRESENT RESEARCH

1. S.C. Yao and Y. Hung, "Analysis of Fluid Flow and Heat Transfer in Heat Exchanger Tube-To-Baffle Clearances," ASME Paper No. 81-WA/HT-10.

2. S.C. Yao, Y.H. Hung, and J. Tang, "Analysis of Dryout in Steam Generator Crevices," ASME Paper No. 81-WA/NE-2.

3. S.C. Yao and Y. Chang, "A Scientific Movie - Visual Study of Boiling in Narrow Gaps with Closed Bottom," Submitted to 7th International Heat Transfer Conference.

4. Y. Chang and S.C. Yao, "Critical Heat Flux in Annular Crevices," under preparation.

CHAPTER 1. INTRODUCTION

Boiling at conventional heat transfer surface has been studied extensively in the past thirty years [1]. However, at the same time, the boiling in confined space has been almost completely neglected. The existing information [2], [3] is limited and incomplete.

In many equipments, boiling occurs in confined space. For example, in the steam generators, clearance is allowed between the heated tube and its support-plate where the tube runs through. In the clearance, flow is reduced and boiling occurs, which is shown in the Fig. 1(a). When the liquid is highly subcooled, single phase forced convection occurs in the crevice. The behavior of the leakage stream, as shown in Fig. 1(b) is of great interest to the designer of heat exchangers. At the tube sheet of steam generator a crevice with closed bottom is formed. The boiling and dryout may also occur in this tube sheet crevice as indicated in the Fig. 1(c).

The boiling of liquid in confined space leads to permanent dryout. Corrosive concentration may build up at the boundary of dryout zone where boiling occurs. Solid deposits may also occur at the dryout boundary. The understanding of the thermal-hydraulic related corrosion in confined space is lacking. This is primary because the boiling heat transfer in confined space is not really known. The fundamental understanding of the boiling heat transfer in confined space is also important to the advances in power engineering and lubrication engineering.

In view of this need, a systematic study of boiling heat transfer in confined space is performed at the Department of Mechanical Engineering of Carnegie-Mellon University under the support of the Office of Naval Research. Both experimental and analytical research are performed.

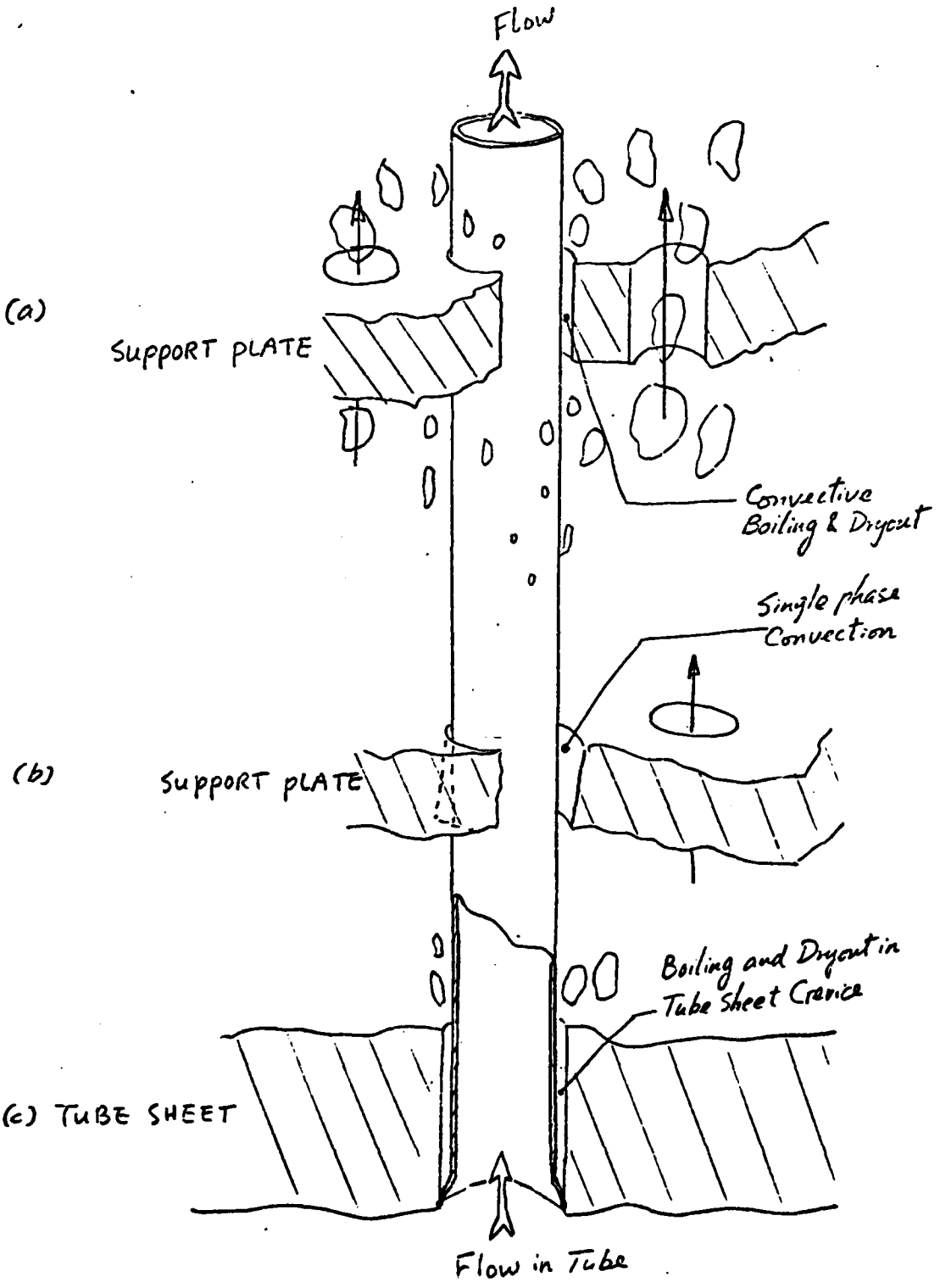
Flow
(a)
SUPPORT PLATE
Convective Boiling & Dryout
Single phase Convection
(b)
SUPPORT PLATE
Boiling and Dryout in Tube Sheet Crevice
(c) TUBE SHEET
Flow in Tube

Fig 1

The progress of the research has been presented in this report in the following chapters:

Chapter 2. Analysis of Single Phase Convection in Support-Plate Crevices.

Chapter 3. Analysis of Convective Boiling and Dryout in Support-Plate Crevices.

Chapter 4. Experiments of Boiling and Dryout in Annular Crevices with Closed Bottoms.

Chapter 5. Experiments of Convective Boiling and Dryout in Annular Crevices.

REFERENCES

1. Tong, L. S., Boiling Heat Transfer and Two-Phase Flow, John Wiley & Sons, 1965.

2. M. Jensen, A. Bergles, and P. Cooper, "Boiling Heat Transfer and Dryout in Restricted Annular Geometries", 16th National Heat Transfer Conference, Paper No. AICHE-14, 1976.

3. E. Ishibashi, and K. Nichikawa, "Saturated Boiling Heat Transfer in Narrow Spaces", Int. J. of Heat Mass Transfer, Vol. 12, pp. 863-94, 1969.

CHAPTER 2
ANALYSIS OF SINGLE PHASE CONVECTION IN SUPPORT-PLATE CREVICES

ABSTRACT

The laminar flow and heat convection in annular type crevices of various eccentricities and inclinations are analyzed. The annulus is heated by hot flowing fluid at the inside of the inner tube. The flow field is calculated using creeping flow approximation of boundary layer theory. The thermal field is studied two-dimensionally in terms of the local bulk mean temperature of the fluid. Calculation is performed numerically but in non-dimensional form. It is observed that the angle of inclination influences the flow and heat transfer significantly especially when the eccentricity is severe. When the angle of inclination increases, the flow rate is reduced, the bulk mean temperature at the exit of crevice increases, and the averaged heat transfer coefficient in crevice decreases. Comparisons are made with respect to the results of concentric annulus.

NOMENCLATURE

A	Cross section area of axial flow in crevice
c	Averaged gap thickness in the crevice
C_p	Specific heat of the fluid in crevice
e	Eccentricity, defined in Figure 1
f	Apparent friction factor for crevice, define in equation (41)
h_i	Heat transfer coefficient inside the tube
h_o	Local heat transfer coefficient at outside of tube in crevice
$\bar{h}$	Averaged heat transfer coefficient on the tube in the whole crevice
H	Local overall heat transfer coefficient from the inside of the tube to crevice defined in equation (17).
k_l	Thermal conductivity of the fluid in crevice
k_s	Thermal conductivity of the tube material
L	The axial length of tube in crevice
$\dot{m}$	The total mass flow rate through the crevice
n	Index of inclination of the tube
Nu*	Characteristic Nusselt number of crevice, defined in equation (38)
$\overline{Nu}$	Averaged Nusselt number in crevice, defined in equation (44)
p	Local pressure of fluid
p_o	Pressure difference across the crevice
P	Non-dimensional pressure defined in equation (24)
Pe*	Characteristic Peclet number of crevice, defined in equation (39)
$\bar{q}_w$	Averaged heat flux of the tube
R	Radius of the tube
s	The thickness of the tube
S	Ratio of the dimensions of the flattened crevice, defined in equation (22)
T	Local temperature of fluid

$\bar{T}$	Local bulk mean temperature of the fluid in crevice
T_i	Bulk mean temperature of hot fluid inside tube
T_o	Temperature of fluid at inlet of crevice
$\bar{T}_e$	Bulk mean temperature of fluid at the exit of crevice
u	Local velocity of fluid in θ direction, a function of z
$\bar{u}$	Local velocity of fluid in θ direction, averaged over the gap
U	Non-dimensional velocity of fluid, in θ direction defined in equation (25)
v	Local axial velocity of fluid, a function of z
$\bar{v}$	Local axial velocity of fluid, averaged over the gap
v^*	Characteristic axial velocity of fluid, defined in equation (40)
V	Non-dimensional axial velocity of fluid, defined in equation (26)
x	Coordinate measured in θ direction
X	Non-dimensional x coordinate, defined in equation (20)
y	Coordinate measured in axial direction
Y	Non-dimensional y coordinate, defined in equation (21)
z	Coordinate measured normal to tube surface across the gap

Greek

α Thermal diffusivity of fluid in crevice

δ Local thickness of gap in crevice

Δ Non-dimensional gap thickness of crevice, defined in equation (23)

ϵ Eccentricity ratio defined in equation (2)

γ Angle, defined in Figure 1

θ Non-dimensional local bulk mean temperature of fluid, defined in equation (27)

μ Viscosity of fluid in crevice

ν Kinematic viscosity of fluid in crevice

ρ Density of fluid in crevice

INTRODUCTION

The fluid flow and heat transfer behavior in concentric annulus are well known [1]. However, in many practical thermal systems the axis of the inner tube may be inclined with respect to the outer shroud. Since the annular gap could be very narrow, if the inner tube is slightly off-centered the periferal variation of the flow channel gap-thickness could be very sévere. The fluid flow and heat transfer in this kind of annular-type-crevices will be relatively complex. In conventional shell-and-tube heat exchangers and steam generators, the hot tube runs through the hole in baffle-plate or support-plate with a narrow mechanical clearance in between of the tube and wall of the hole. Due to the misalignment of the plates and the displacement of tube in the flow field it is likely that the tube may be inclined in the hole to form an inclined annular-type crevice.

The flow is forced through the crevice by the pressure difference across the plate. The fluid is also heated by the hot tube in the crevice. The knowledge of the flow rate and temperature of the leakage stream is of great importance to the understanding of the thermal performance of these heat exchange equipments. This type of heat transfer problems also occur in many other industrial applications.

The analysis of the fluid flow in concentric annular orifices has been reported in references [2,3]. The fluid mechanic study of annuli of small clearances has also been performed in references [4,5] for concentric and eccentric configurations. However, no analysis has been conducted for the general case of annular-type crevices with the inner tube inclined and placed eccentrically. The analysis of the flow in this generalized condition is one of the objectives of the present study.

The other objective of the present study is to analyze generally the convective heat transfer in annular-type crevices. In most applications the tube is heated from inside by another flowing hot fluid such that the outside surface condition of the tube is neither at a constant heat flux nor at a constant temperature. The heat transfer of eccentric annulus at constant heat flux has been studied in [6] for slug flow. However, no analysis has been performed for laminar flow in annular-type crevices with inclined inner tube. In fact, this information is of great importance to the heat exchanger designs [7].

In the following sections the fluid flow and heat convection of annular-type-crevices will be analyzed. To limit the complexity of the problem the following assumptions were made:

(1) The problem is steady state with constant properties for the fluid.

(2) The flow is laminar in the crevice with negligible inertial effect and negligible energy dissipation. The entrance effects are neglected.

(3) Heating is provided by the hot fluid in the tube. The tube is generally not in contact with the shroud. Should contact occur, the contact will be limited to a point.

FORMULATION

Geometry: To describe the geometry of the annular-type-crevices accurately the local gap thickness of the flow channel has to be quantified. At any cross-sectional cut view of the crevice the configuration of the flow channel can be described as an eccentric annulus. For two eccentric circles with eccentricity e and with their radii having a small difference c, the gap thickness δ can be evaluated accurately but not exactly from Figure 1 as

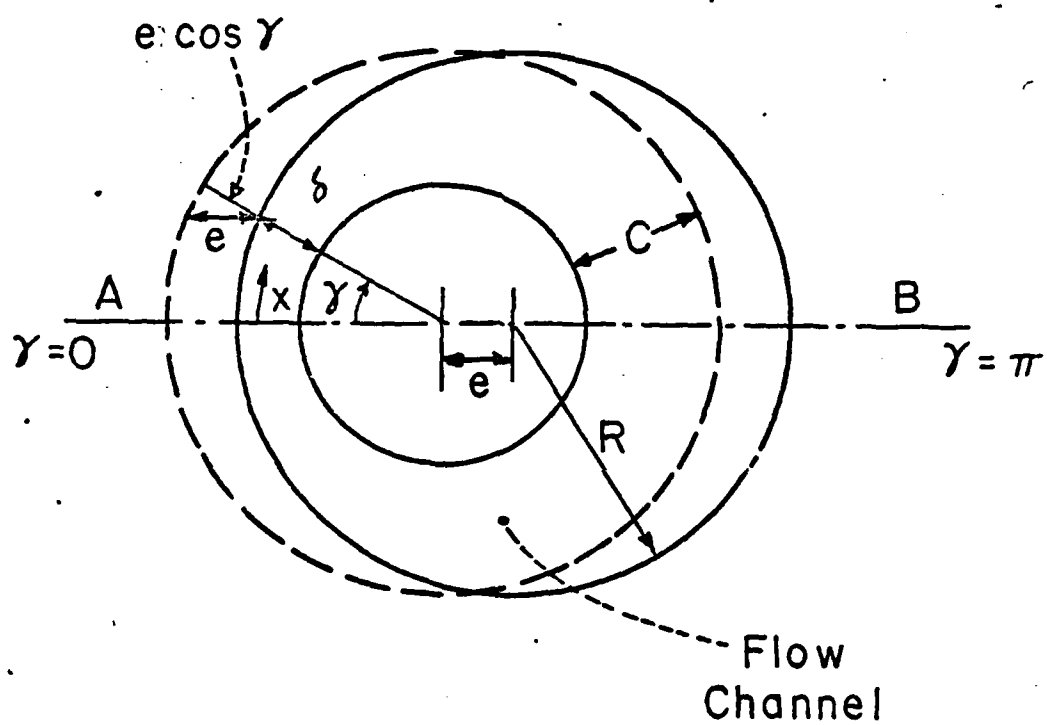

$$\delta(\gamma) = C\,(1 - \epsilon \cos\gamma)$$

Fig. 1. **The Bottom View of Eccentric Annulus**

$$\delta(\gamma) = c(1-\varepsilon \cos \gamma) \tag{1}$$

where
$$\varepsilon = e/c \tag{2}$$

is the eccentricity ratio which varies between 0 and 1.

If the inner tube is inclined with respect to the outer shroud, the eccentricity ratio ε would be a function of the axial location. The displacement of the inner tube can be decomposed as two steps. First, the tube moves from the concentric position to an eccentric position. Then the tube is inclined with an angle. In the present study, a simple but typical condition is considered that the plane of inclination of the inner tube passes through the center line of the outer shroud. This is shown in Figure 2. The general formulation for the gap of crevice is

$$\delta = c\{1-\varepsilon[1- 2n(1-(y/L))] \cos \gamma\} \tag{3}$$

where the eccentricity ratio ε is the value at the cross-section where $y = L$. The n, called the index of inclination, controls the angle of inclination of the inner tube. When n equals zero the inner tube is in parallel with the outer shroud. At this moment the equation (3) is the same as equation (2). When the n increases but with the ε fixed, the anlge of inclination of the tube increases while its relative position at $y = L$ is not changed. When n equals unity, the inner tube inclines symmetrically in the crevice from a side view. For the extreme condition of $\varepsilon = 1$ and $n = 1$, the inner tube contacts the outer shroud at two points $y = 0$ and $y = L$ respectively.

The cross-sectional view of the crevice, as shown in Figure 1, is symmetric with respect to the line A-B. Therefore, only half of the total crevice has to be calculated. In the present study the gap thickness δ is generally much smaller than the tube radius R such that the curvature

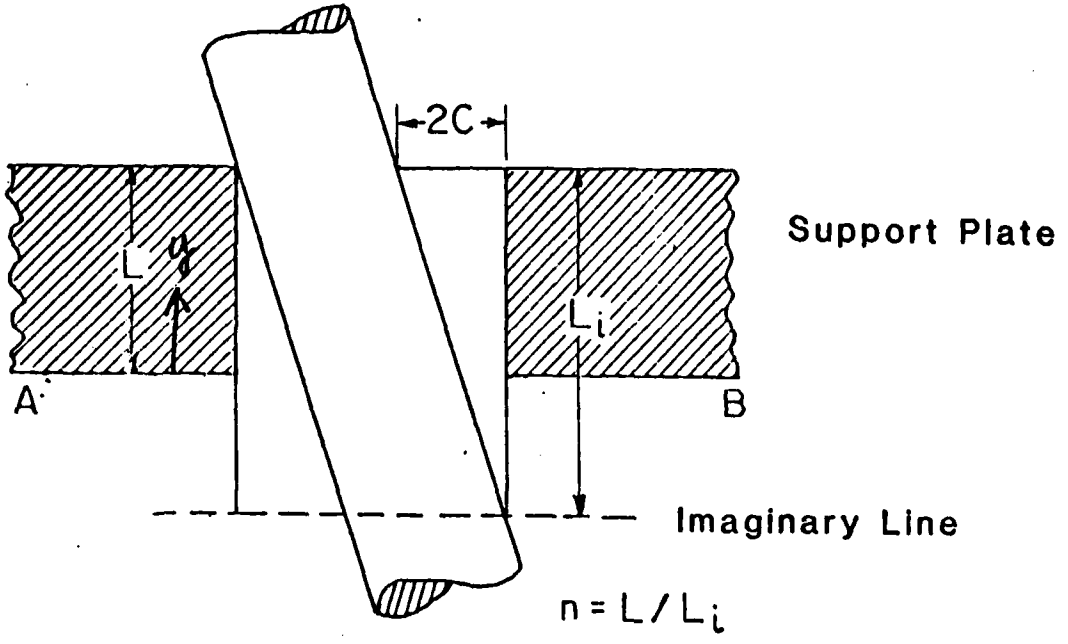

$$\delta(x,y) = C\left\{1-\epsilon\left[1-2n\left(1-\frac{y}{L}\right)\right]\cos\gamma\right\}$$

Fig. 2. The Side View of An Inclined Annular Crevice

of the crevice can be neglected. Therefore, the crevice can be analyzed as a flattened channel with the varying height δ as shown schematically in Figure 3. The dimension of the flat channel is L in the y direction and πR in the x direction with a local height $\delta(xy)$. The symmetry conditions will be applied to the lines of $x = 0$, and $x = \pi R$.

Flow Field: The creeping flow approximation to the boundary layer theory will be applied to the annular-type crevices. For the laminar flow in narrow flow passage, the flow field will be dominated by the viscous force and the pressure driving-force. The fluid inertia force may be neglected [8] if

$$\frac{v^* L}{\nu} \left(\frac{c}{L}\right)^2 << 1 \tag{4}$$

where the v^* is the characteristic velocity of fluid in the crevice and will be defined later. At this condition the velocity profiles become parabolic. The parabolic velocity profiles can be substituted into the equation of continuity and integrated cross the gap from 0 to δ. The result is

$$\frac{\partial}{\partial x} \left(\delta^3 \frac{\partial p}{\partial x}\right) + \frac{\partial}{\partial y} \left(\delta^3 \frac{\partial p}{\partial y}\right) = 0 \tag{5}$$

which is the Reynold's equation of lubrication [8] when the walls are not in motion. In this equation the δ is given from the known geometry of crevice and the pressure field is unknown. The boundary conditions are

$$p(x, 0) = p_o \tag{6}$$

$$p(x, L) = 0 \tag{7}$$

where the p_o is the driving pressure over the crevice, and

$$\frac{\partial p}{\partial x} (0, y) = 0 \tag{8}$$

$$\frac{\partial p}{\partial x} (\pi R, y) = 0 \tag{9}$$

for the symmetry condition as described previously.

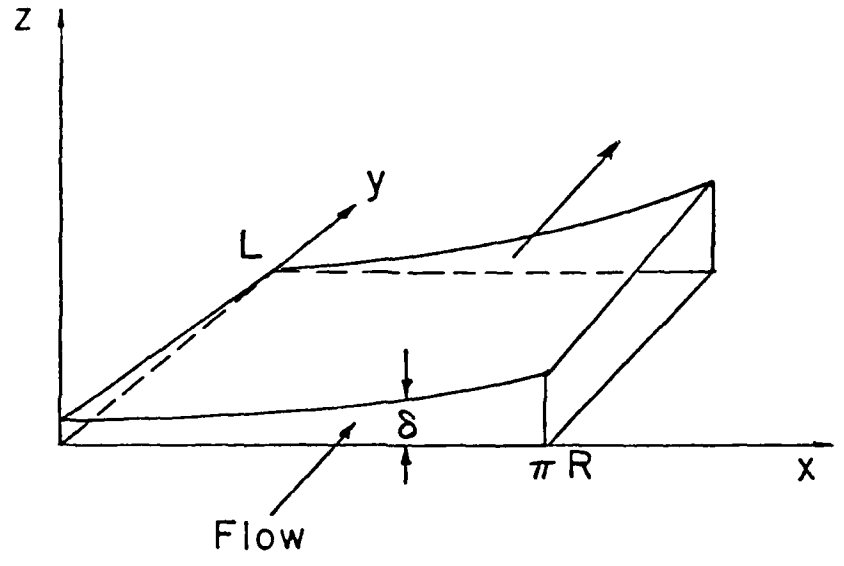

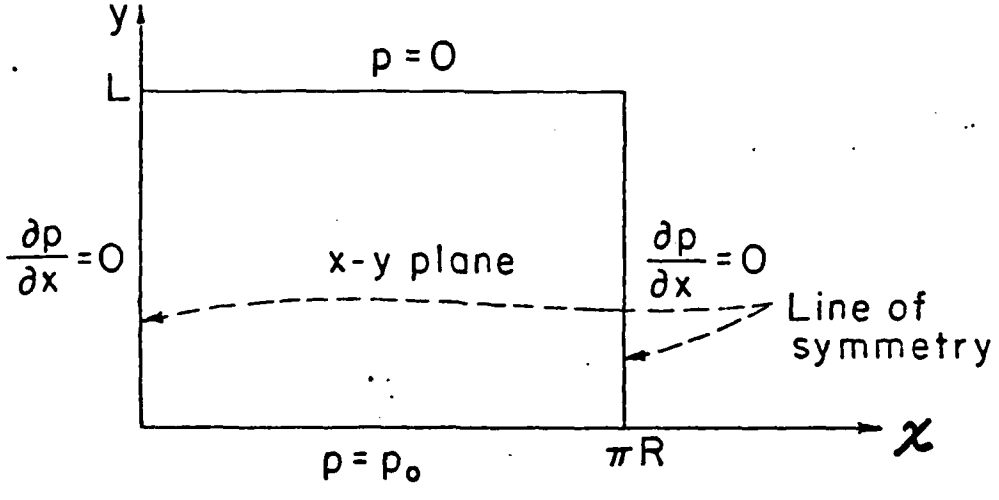

Typical Geometry of the Crevice Considered in Analysis

Fig. 3.

Once the pressure field has been solved, the "averaged" fluid velocity of the parabolic profile can be evaluated from

$$\bar{u} = -\frac{1}{12\mu}\frac{\partial p}{\partial x}\,\delta^2 \tag{10}$$

$$\bar{v} = -\frac{1}{12\mu}\frac{\partial p}{\partial y}\,\delta^2 \tag{11}$$

Heat Transfer: Considering the constant properties and neglecting the viscous dissipation, the energy equation of the laminar flow in the crevice becomes

$$u\frac{\partial T}{\partial x} + v\frac{\partial T}{\partial y} = \alpha\left(\frac{\partial^2 T}{\partial x^2} + \frac{\partial^2 T}{\partial y^2} + \frac{\partial^2 T}{\partial z^2}\right) \tag{12}$$

The order of magnitude analysis can be performed to justify the importance of each term. Normalize the velocity by v*, x and y by L, and z by δ. The convective terms are of the order 1; the conduction in x and y directions are of the order $(v^* L/\alpha)^{-1}$; and the conduction in z direction becomes order of $[(v^*L/\alpha)(\delta/L)^2]^{-1}$. Considering the criterion in equation (4) and assuming the Prandtl number of the order 1, the conduction in z direction would be dominant. The conduction in x or y direction would be negligible because the characteristic Peclet number (v^*L/α) is generally much larger than one. The omitting of the conduction in x and y direction is further supported by the particular type of heating condition in the present study. The temperature of the hottest point in the crevice is limited by the hot fluid temperature in the tube; therefore, a severe hot spot is not likely to occur and the conduction in x or y direction will be limited too.

The remaining energy equation can be integrated with respect to z from 0 to δ and gives

$$\int_0^{\delta} u \frac{\partial T}{\partial x}\, dz + \int_0^{\delta} v \frac{\partial T}{\partial y}\, dz = \alpha \frac{\partial T}{\partial z} \Big]_0^{\delta} \tag{13}$$

Following the derivation in the Appendix, the first term of the equation (13) can be written as

$$\int_0^{\delta} u \frac{\partial T}{\partial x}\, dz = \delta \bar{u} \frac{\partial \bar{T}}{\partial x} - \int_0^{\delta} \frac{\partial u}{\partial x} (T - \bar{T})\, dz \tag{14}$$

where the $\bar{T}$ is the local bulk mean temperature of the fluid. Since the gap of the crevice is narrow, the local temperature of fluid is very close to the local bulk mean temperature. When the gap thickness δ does not vary strongly in the crevice, the value of $\partial u/\partial x$ will also be small. Therefore the last term in the equation (14) can be neglected in general. Approximate the second term in equation (13) in the same manner, the energy equation becomes

$$\bar{u}\, \delta \frac{\partial \bar{T}}{\partial x} + \bar{v}\, \delta \frac{\partial \bar{T}}{\partial y} = \alpha \frac{\partial T}{\partial z} \Big]_0^{\delta} \tag{15}$$

If the crevice is heated from the inner tube and insulated at the outer tube, the last term in the equation (15) can be written as $q_w/\rho C_p$. The wall heat flux q_w can be described as $H(T_i - \bar{T})$. Therefore the energy equation is

$$\bar{u} \frac{\partial \bar{T}}{\partial x} + \bar{v} \frac{\partial \bar{T}}{\partial y} = \frac{H}{\delta(xy)\rho C_p} (T_i - \bar{T}) \tag{16}$$

where the H is the overall heat transfer coefficient defined as

$$\frac{1}{H} = \frac{1}{h_i} + \frac{s}{k_s} + \frac{1}{h_o} \tag{17}$$

The energy equation (16) is a first order linear partial differential equation of the hyperbolic form. The initial conditions are

$$\bar{T}\Big|_{y=0} = T_o \quad \text{at inlet, and} \tag{18}$$

$$\frac{\partial \bar{T}}{\partial x}\Big|_{x=0} = 0 \quad \text{for the symmetry.} \tag{19}$$

Non-Dimensionalization: The parameters can be non-dimensionalized using

$$X = \frac{x}{\pi R} \tag{20}$$

$$Y = \frac{y}{L} \tag{21}$$

$$S = \frac{L}{\pi R} \tag{22}$$

$$\Delta = \frac{\delta}{c} \tag{23}$$

$$P = \frac{p}{p_o} \tag{24}$$

$$U = \frac{\mu \bar{u} \pi R}{p_o c^2} \tag{25}$$

$$V = \frac{\mu \bar{v} L}{p_o c^2} \tag{26}$$

and

$$\theta = \frac{\bar{T} - T_o}{\bar{T}_i - T_o} \tag{27}$$

Then the Reynold's equation and the boundary conditions become

$$S^2 \frac{\partial}{\partial X}\left(\Delta^3 \frac{\partial P}{\partial X}\right) + \frac{\partial}{\partial Y}\left(\Delta^3 \frac{\partial P}{\partial Y}\right) = 0 \tag{28}$$

with

$$P(X,0) = 1 \tag{29}$$

$$P(X,1) = 0 \tag{30}$$

$$\frac{\partial P}{\partial X}(0,Y) = 0 \tag{31}$$

$$\frac{\partial P}{\partial X}(1,Y) = 0 \tag{32}$$

The non-dimensional velocity field is described by

$$U = -\frac{1}{12}\Delta^2 \frac{\partial P}{\partial X} \tag{33}$$

$$V = -\frac{1}{12}\Delta^2 \frac{\partial P}{\partial Y} \tag{34}$$

The energy equation and its initial conditions are

$$S^2 U \frac{\partial \theta}{\partial X} + V \frac{\partial \theta}{\partial Y} = \frac{1}{\Delta}\left(\frac{L}{c}\right)\left(\frac{Nu^*}{Pe^*}\right)(1-\theta) \tag{35}$$

with

$$\theta = 0 \quad \text{at} \quad Y = 0 \tag{36}$$

$$\frac{\partial \theta}{\partial X} = 0 \quad \text{at} \quad X = 0 \tag{37}$$

where

$$Nu^* = \frac{H2c}{k_1} \tag{38}$$

$$Pe^* = \frac{v^* 2c}{\alpha} \quad , \text{ and} \tag{39}$$

$$v^* = \frac{P_o c^2}{\mu L} \tag{40}$$

the v* is the characteristic axial velocity in the crevice at laminar flow.

NUMERICAL METHOD

The pressure field is calculated from the Reynold's equation of lubrication as shown in equations (28) to (32). To solve this Poisson equation, the method of Alternative Directional Implicit numerical scheme [9] is used. The implicit calculations are performed along horizontal lines for the whole region of the flow field; then the calculations are performed along all the vertical lines alternatively. In the implicit scheme of the solution along a line the method of Gauss Elimination is used to solve the system of equations.

The thermal field is then calculated using the known velocity field which is derived from the pressure field. In solving the energy equation the upwind-difference scheme[10] has been used to maintain a stable numerical computation.

The whole field is typically discretized into 20 x 18 meshes. Approximately 20 iterations are required in the Alternative Directional Implicit calculations to reach a converged solution. The result is validated with hand calculations. The overall computer time for the calculation is about 12 cpu seconds using a DEC-20 computer.

RESULTS AND DISCUSSION

To illustrate the result of fluid flow and heat transfer calculations, a specific example is studied in detail. The inner tube contacts with the outer shroud at the top but with a small angle of inclination. Fluid flows upward in the crevice. The calculated pressure field is shown in Figure 4 in non-dimensional form. The geometric configuration of the crevice is also specified in this figure. The pressure field is distorted and the flow stream diverts from the point of contact where the gap thickness is the minimum.

For the same crevice, the thermal field is shown in Figure 5 in non-dimensional form. Since the gap is wide at the location where the X is large, the flow is faster over there and the local bulk mean temperature rises relatively slow along the stream. In the region where X is small, the flow is retarded due to the narrow gap thickness. The fluid temperature rises fast and reaches the temperature of hot fluid inside the tube in a short distance. This high temperature region is relatively large in this example. If the inner tube is not in contact with the outer shroud, the hot region would be small or inexist.

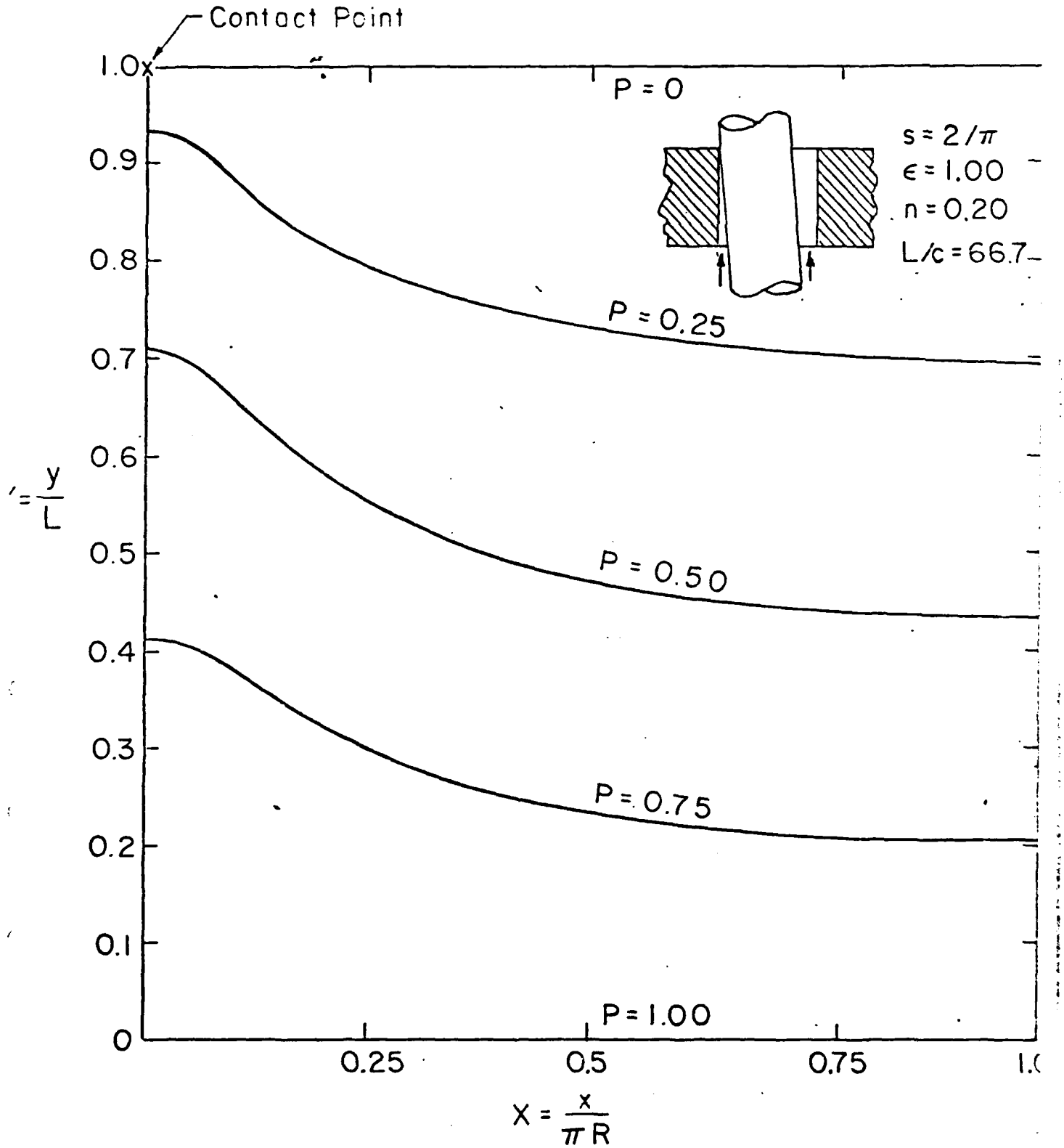

Fig. 4. The Pressure Distribution for 1-point Contact Crevice

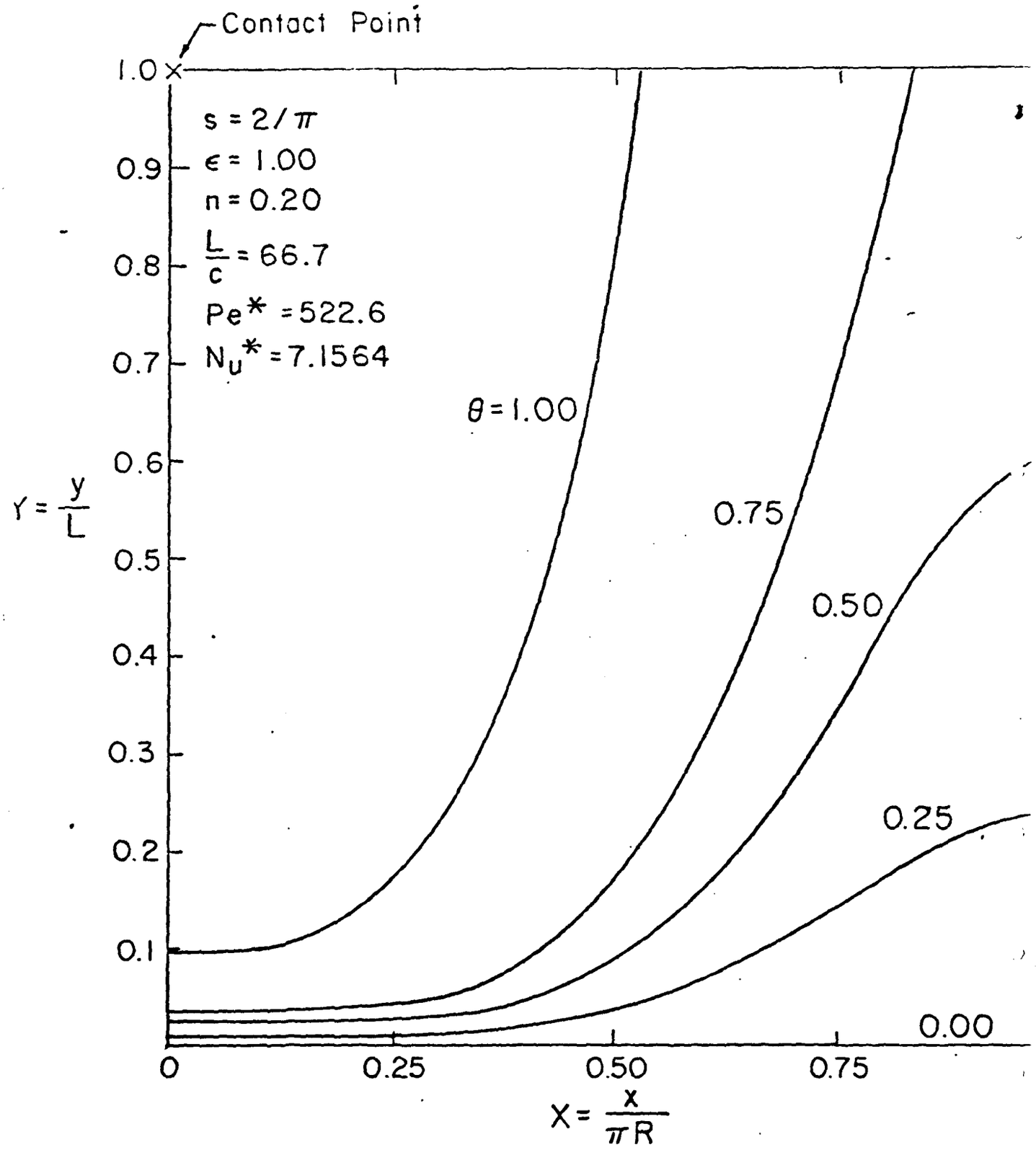

Fig. 5. The Isotherm Map for 1-point Contact Crevice With Constant Bulk Mean Temperature Inside the Tube

Many other cases are studied for various eccentricity ratio ε and inclination index n for this crevice. The parameters of this crevice has been listed in Table 1. For the same crevice, the ratio of the mass flow rates at various conditions and the mass flow rate at concentric configuration are shown in Figure 6 with the eccentricity ratio ε as horizontal coordinate and the inclination index n as parameter. When n equals zero the tube is in parallel to the shroud. As indicated in Figure 6, at a fixed ε the more the inclination (i.e., higher value of n) the lower the mass flow rate. This is because the flow streams are distorted when the tube is inclined in the crevice. The extreme conditions occur when ε equals unity, where the inner tube contacts the outer shroud at the top edge. When n equals zero, the tubes have a line of contact with shroud in crevice. Large amounts of fluid passes through the wide opening at the other side of the crevice and gives the highest possible mass flow rate in all the configurations (2.5 times that of concentric annulus). If n equals unity, the tubes has two contact points at the top and bottom of crevice respectively. The mass flow rate at this condition is the lowest of all the cases studied (about 70 percent of the concentric annulus).

The overall flow resistance of the crevice can be characterized by an "apparent" friction factor which is defined in a conventional manner as

$$\Delta p = f\left(\frac{L}{2c}\right) \frac{1}{2} \frac{\dot{m}^2}{\rho A^2} \tag{41}$$

It is interesting to point out that for a crevice with fixed dimensions the total cross-sectional area A of the flow is a constant value irrespective to the eccentricity of the tube in the crevice. The apparent friction factor of the crevice is shown in Figure 7 for various ε and n. The Reynolds number here is based upon the area averaged axial velocity of the fluid in crevice. The nature

TABLE 1

PARAMETERS OF THE CREVICE STUDIED HERE

S	L/c	Pe*	Nu*
$\frac{2}{\pi}$	66.7	522.6	7.156

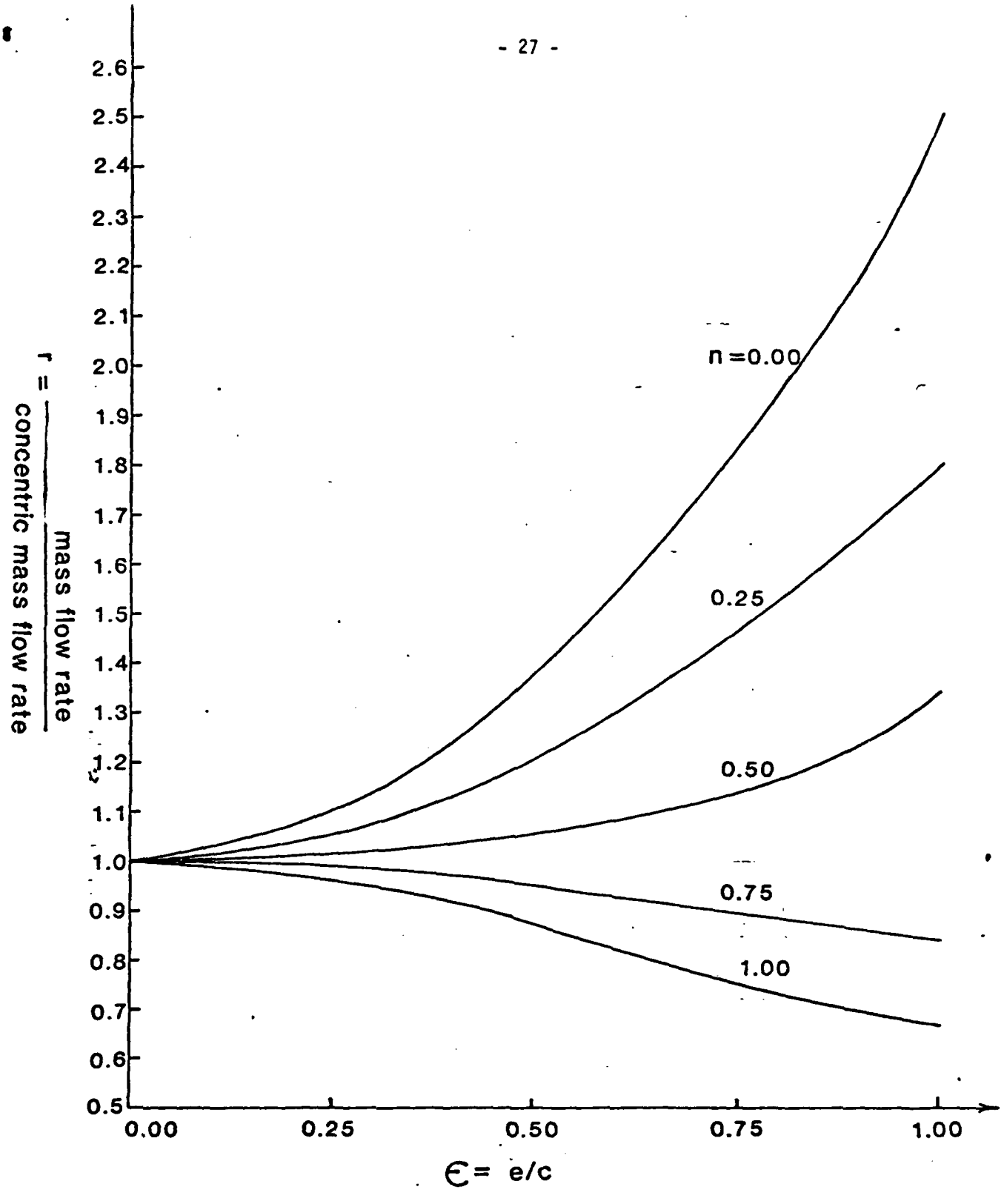

Fig. 6. Flow ratio versus eccentricity ratio in laminar flow

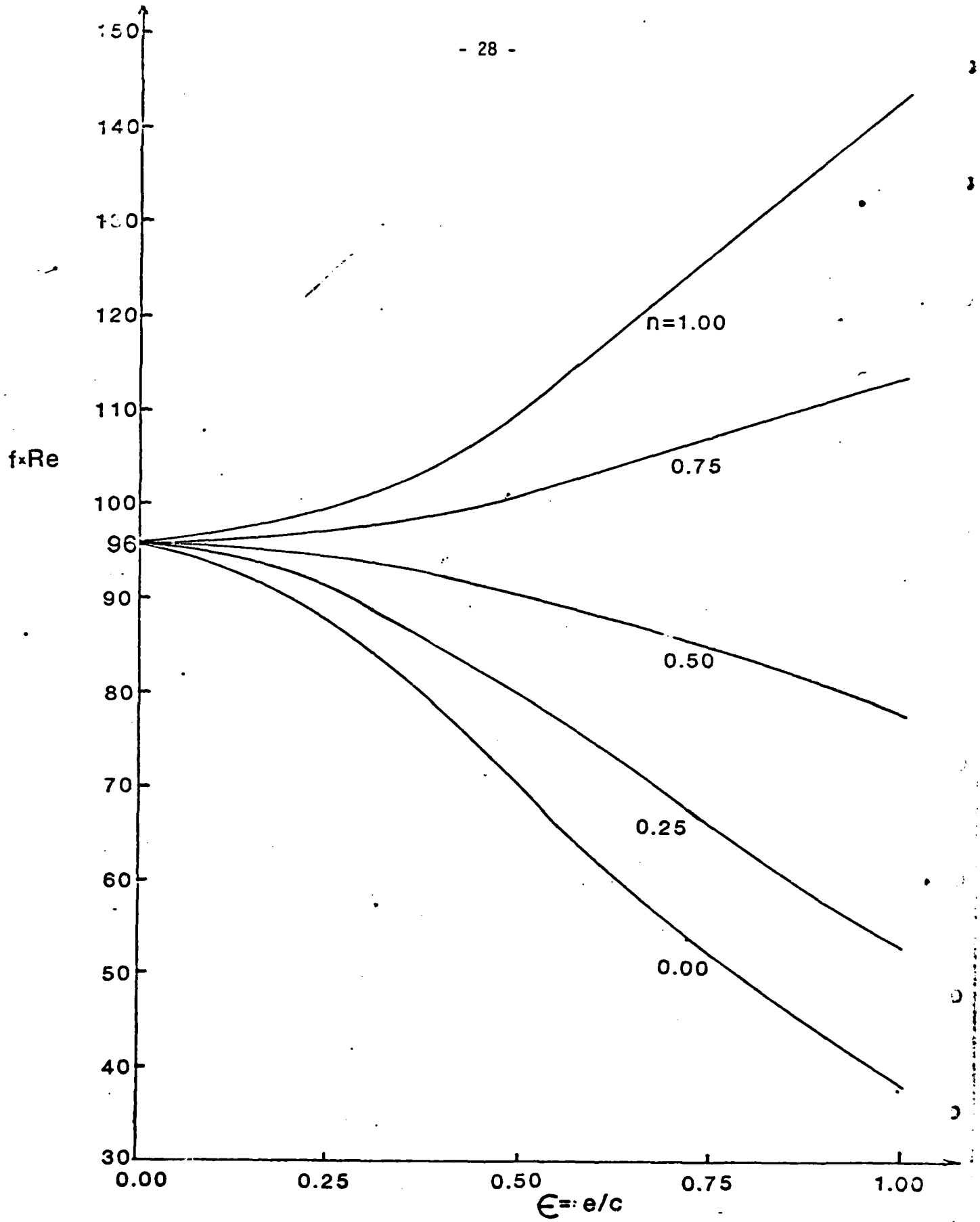

Fig. 7. Apparent friction coefficient versus [illegible] in laminar flow

of this figure is similar to that of Figure 6 due to their interrelationship in equation (41).

The non-dimensional bulk mean temperature of the leakage stream leaving the crevice is shown in Figure 8 for various values of ε and n. The condition of heating is described in Table 1. When the tubes are concentric (ε=0) the leakage is as hot as the temperature of fluid in the tube. If the leakage stream is more (for example, ε>0.5 but n < 0.5) the temperature of the leakage stream becomes lower. However, when the inner tube is further inclined with the n value equals or larger than 0.75 the leakage stream could be equal or less than that of concentric annulus (see Figure 6) the temperature of leakage stream will be as hot as the fluid temperature inside the tube.

Based upon the above information on flow rate as well as temperature of the leakage stream, the averaged heat transfer from the hot tube in the crevice can be evaluated. We may define the averaged heat transfer coefficient as

$$\bar{q}_w = \bar{h}(T_i - T_o) \tag{42}$$

By energy conservation for the whole crevice, the averaged heat flux is

$$\bar{q}_w = \frac{\dot{m}\, C_p(\bar{T}_e - T_i)}{2\pi RL} \tag{43}$$

Therefore the averaged Nusselt number in the crevice can be calculated.

$$\bar{Nu} = \frac{C_p\, c \quad \dot{m}\, \bar{\theta}_e}{\pi\, R\, L\, k_1} \tag{44}$$

The averaged Nusselt numbers of crevice with various geometric configurations are shown in Figure 9 as a ratio to the Nusselt number of concentric annulus. It is interesting to notice that for the condition of present study, the configurations with n < 0.5 gives higher heat transfer coefficient although the

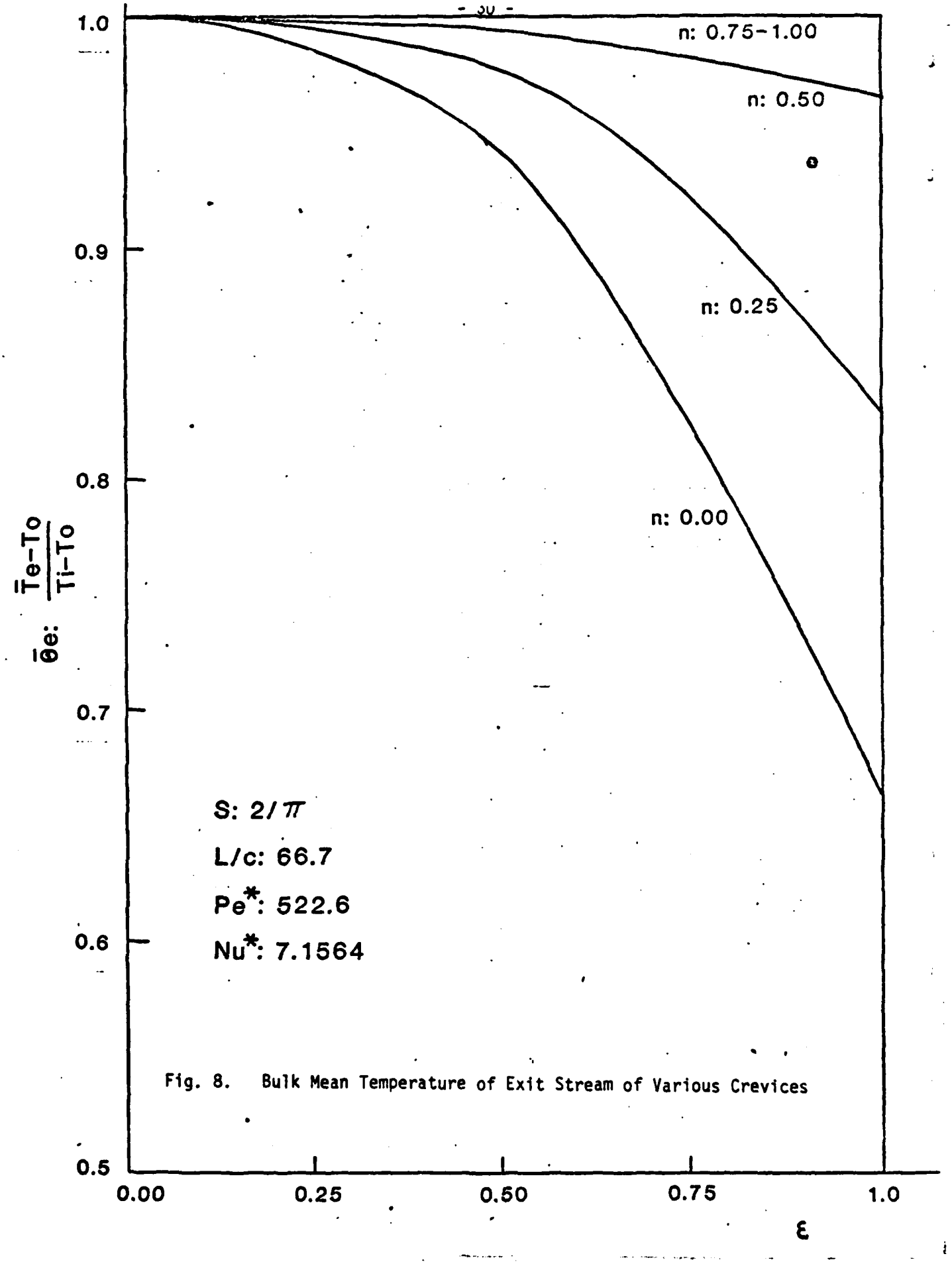

Fig. 8. Bulk Mean Temperature of Exit Stream of Various Crevices

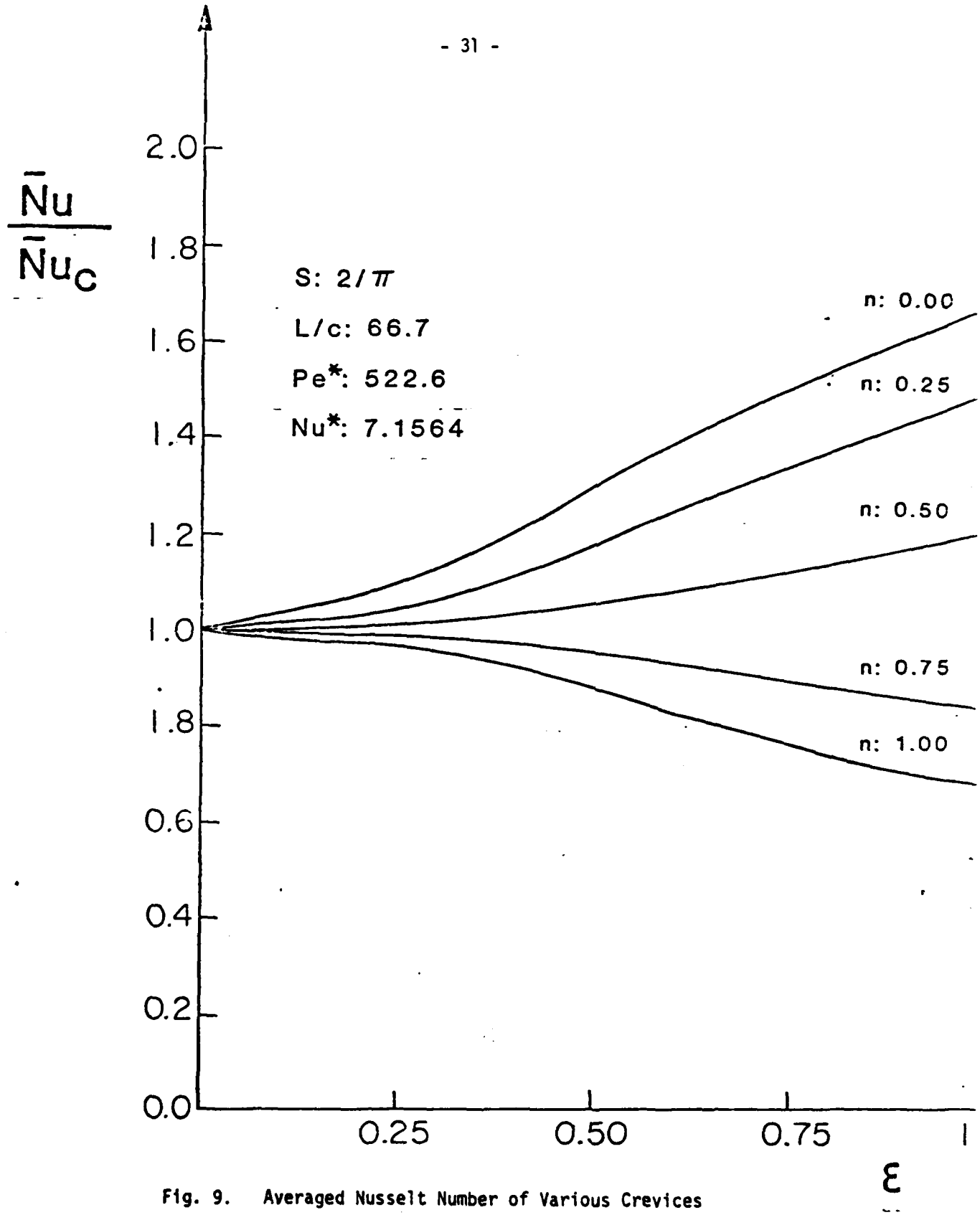

Fig. 9. Averaged Nusselt Number of Various Crevices

bulk mean temperature of the exit stream, as shown in Figure 8, is not as hot as the temperature of fluid inside the tube. This is mainly due to the high flow rate at these conditions as indicated in Figure 6. The $\overline{Nu}$ is essentially related with the product of mass flow rate and exit bulk mean temperature as stated in the equation (44).

CONCLUSION

The laminar flow and heat transfer in annular-type crevices of various geometric configurations are studied in detail. The flow field can be calculated using creeping flow approximation. The thermal field can be formulated in two dimension based upon the local bulk mean temperature in crevice. Comparing with the behavior of concentric annulus, the eccentric annulus with little inclination of the inner tube gives higher mass flow rate, lower bulk mean temperature at exit, but higher averaged heat transfer coefficient in crevice. If the angle of inclination is large, the behavior is reversed. It is suggested that the fluid flow and heat transfer behavior of confined geometry with other types of configurations can also be analyzed in a similar manner.

REFERENCES

1. Kays, W.M., CONVECTIVE HEAT AND MASS TRANSFER, McGraw-Hill, 1966.

2. Bell, K.J., and Bergelin, O.P., "Flow Through Annulus Orifices," Trans. ASME, Vol.79, pp.593-601, 1957.

3. Snyder, W.T., and Goldstein, G.A., "Analysis of Fully Developed Laminar Flow in an Eccentric Annulus," AIChE.J. Vol.11, No.3, pp.462-467, 1965.

4. Nootbaar, R.F., and Kintner, R.C., "Fluid Friction in Annuli of Small Clearance," Proceedings of Second Midwestern Conference of Fluid Mechanics, Ohio State University, Eng. Exp. Station, Bulletin No.149, pp.185-199, 1952.

5. Tao, L.N., and Donovan, W.F., "Through-Flow in Concentric and Eccentric Annuli of Fine Clearance With and Without Relative Motion of the Boundaries," Trans. ASME, Vol.77, pp.1291-1301, 1955.

6. Snyder, W.T., "An Analysis of Slug Flow Heat Transfer in an Eccentric Annulus," AIChE. Journal, Vol.9, No.4, pp.503-506, 1963.

7. Palen, J.W., and Taborek, J., "Solution of Shell Side Flow Pressure Drop and Heat Transfer by Stream Analysis Method," CEP Symp. Series, Vol.65, No.92, pp.53-63, 1969.

8. Schlichting, H., BOUNDARY-LAYER THEORY, McGraw-Hill, p.109, 1968.

9. Carnahan, B., Luther, M.A., Wilkes, J.O., APPLIED NUMERICAL METHODS, John Wiley and Sons, Inc., 1969.

10. Patankar, S.V., NUMERICAL HEAT TRANSFER AND FLUID FLOW, McGraw-Hill, 1980.

APPENDIX A

The Derivation of Equation (14)

Following the definition of average velocity and bulk mean temperature, we get

$$\bar{u}\,\frac{\partial \bar{T}}{\partial x} = \left(\frac{\int_0^\delta u\,dz}{\delta}\right)\,\frac{\partial}{\partial x}\left[\frac{\int_0^\delta u\,T\,dz}{\int_0^\delta u\,dz}\right] \qquad \text{(A-1)}$$

$$= \frac{1}{\delta}\left[\frac{\partial}{\partial x}\int_0^\delta u\,T\,dz - \frac{\int_0^\delta u\,T\,dz}{\delta}\,\frac{\partial}{\partial x}\int_0^\delta u\,dz\right] \qquad \text{(A-2)}$$

$$= \frac{1}{\delta}\left[\frac{\partial}{\partial x}\int_0^\delta u\,T\,dz - \bar{T}\,\frac{\partial}{\partial x}\int_0^\delta u\,dz\right] \qquad \text{(A-3)}$$

use Lebnitz's rule for both of the integrals

$$\bar{u}\,\frac{\partial \bar{T}}{\partial x} = \frac{1}{\delta}\left\{\left[\int_0^\delta u\,\frac{\partial T}{\partial x}\,dz + \int_0^\delta T\,\frac{\partial u}{\partial x}\,dz + u(\delta)\,T(\delta)\,\frac{\partial \delta}{\partial x} - 0\right]\right.$$

$$\left. - \bar{T}\left[\int_0^\delta \frac{\partial u}{\partial x}\,dz + u(\delta)\,\frac{\partial \delta}{\partial x} - 0\right]\right\} \qquad \text{(A-4)}$$

when the non-slip condition for velocity at δ is used this equation becomes

$$\delta\bar{u}\,\frac{\partial \bar{T}}{\partial x} = \int_0^\delta u\,\frac{\partial T}{\partial x}\,dz + \int_0^\delta \frac{\partial u}{\partial x}\,(T - \bar{T})\,dz$$

CHAPTER 3

ANALYSIS OF CONVECTIVE BOILING AND DRYOUT IN SUPPORT-PLATE CREVICES

ABSTRACT

Two-dimensional analysis is performed for the two-phase thermal-hydraulics in annular-type clearances between the heated tube and the support plate in steam generators assuming the fluid is homogeneous, non-slip, and with uniform axial pressure gradient. Numerical computation has been performed for this pressure-boundary problem, using an under-relaxation method for initial iterations to suppress possible numerical instability.

Annular-type clearances with various eccentricities and inclinations are studied. The boiling and dryout pattens at various conditions are presented and compared with available experimental data. The effect of the difference in radii of curvatures near the contact location to the dryout is studied. Recommendation for better design to avoid excessive dryout and corrosion is proposed.

NOMENCLATURE

c	the average gap thickness of the crevice
D_h	hydraulic diameter, equals 2h for parallel plates
f	friction factor of the liquid at the same mass flow rate
G_x	local cross mass flux
Gy	local axial mass flow rate per unit flow cross section area, this is local axial mass flux
h	local gap thickness of crevice
h_s	heat transfer coefficient in the crevice
h_t	heat transfer coefficient in the tube
H	local enthalpy of fluid
H_{fg}	latent heat of evaporation
$H_{l,sat}$	enthalpy of saturated liquid
m	total mass flow rate in y direction in the whole crevice
n	inclination index
p	pressure
p_o	total pressure difference
q_w	wall heat flux into the crevice
r	ratio of cross flow to axial flow, based on mass flow
R	radius of the tube
T	local temperature of fluid, average over gap thickness
T_t	bulk mean temperature in the tube
x	coordinate
y	coordinate in axial direction.

Greek Symbols

β	local fluid quality

δ	thickness of the tube
ϵ	eccentricity, defined after equation (1)
θ	angle, as shown in Figure 2
ρ	density of the fluid (single phase or two phase)
ρ_l	density of liquid
Φ	two phase friction multiplier based on f_l

INTRODUCTION

In many tube-and-shell steam generators the heated tubes are fixed in space by support-plates. As shown in Figure 1, holes are drilled in the support-plate to allow the tubes to pass through. Mechanical clearance is provided between the tube and the support-plate. Due to the narrow passage of the clearance, fluid flows slowly in it. When the tube temperature is higher than the saturation temperature of the fluid at the shell-side, boiling and possibly permanent dryout may occur in the crevices. Corrosive concentrations build up at the boundary of the dryout zone where solid deposits may also appear. In fact, corrosion and denting of tubes has been observed frequently at the support-plate crevices in many steam generators.

Analysis has been performed to predict the dryout pattern in crevices [1]; however, the analysis is limited to one-dimensional flow where no cross-flow is allowed in the azimuthal direction. Practically, when the axis of the tube is not in parallel to the axis of the hole on the support plate, the flow in the crevice will have an azimuthal component. In some cases, the tube may contact the wall of the support-plate hole. Near the contact location flow is greatly retarded, and boiling occurs easily. The vapor generated from the local boiling will also have a tendency to push the adjacent fluid away in the azimuthal direction and induces cross-flow. For a better modeling, two-dimensional calculation is desired. In this paper the boiling and dryout in crevices are calculated following an approach of subchannel analysis which has been used widely in tube bundle thermal hydraulic analysis.

The knowledge of thermal-hydraulic phenomena in tube bundles has been greatly advanced in the last decade. A number of subchannel computer programs have been developed, for example, in references [2-3]. Invariably, most of these methods require the evaluation of empirical constants, usually by comparison with

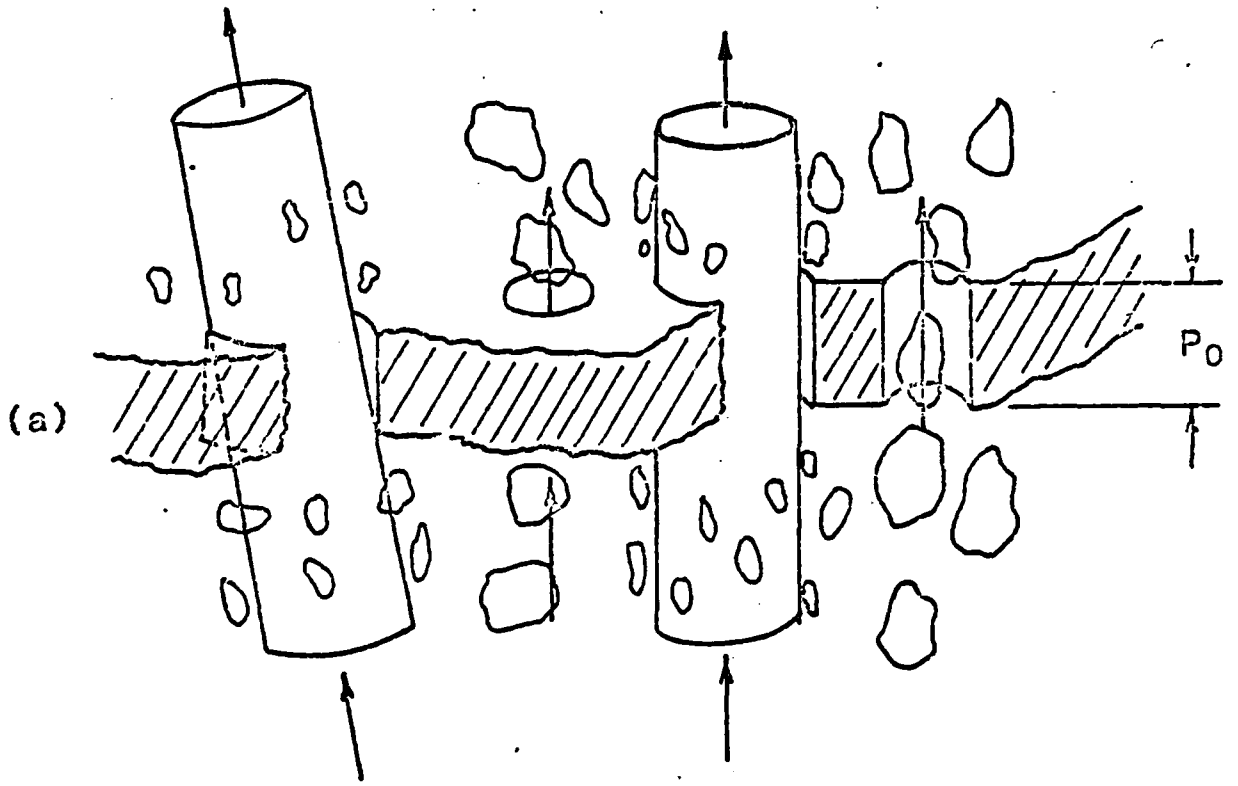

Fig. 1. The relation of tube and the support-plate.

experimental data, before quantitative predictions can be made. The considered transport mechanisms consist of turbulent mixing, thermal conduction, diversion cross flow, etc. Attempts have been made to use subchannel programs to evaluate the dryout in crevices. Numerical instability prohibits successful calculation.

In view of the particular feature of the crevices, some simplifications can be made to the subchannel calculation. The narrow crevice suppresses the communication between subchannels. The turbulent mixing and the thermal conduction among subchannels can be neglected with respect to the diversion cross flow and the heat transfer at wall respectively. The use of empirical constants in calculation is also undesirable due to lack of knowledge on the physical behavior in crevices. Therefore, an appr ximate but effective calculation method is proposed based upon the principles which have been used in the SIMPLE II Program [4]. Simplifications have been made to this computer program but with the extension to two phase heat transfer. Other assumptions and the derivations of the analysis will be presented in a latter section. The method used to suppress the numerical instability will also be discussed later.

GEOMETRY

To describe the geometry of the annular-type crevices accurately the local gap thickness of the flow channel has to be quantified. At any cross-sectional cut view of the crevice the configuration of the flow channel can be described as an eccentric annulus. For two eccentric circles with eccentricity e and with their radii having a small difference c, the thickness δ can be evaluated accurately but not exactly from Figure 2 as

$$h(\theta) = c(1-\epsilon \cos\theta) \text{ , where} \quad (1)$$

$$\epsilon = e/c \quad (2)$$

is the eccentricity ratio which varies between 0 and 1.

If the inner tube is inclined with respect to the outer shroud, the eccentricity ratio ϵ would be a function of the axial location. The displacement of the inner tube can be decomposed as two steps. First, the tube moves from the concentric position to an eccentric position. Then the tube is inclined with an angle. In the present study, a simple but typical condition is considered that the plane of inclination of the inner tube passes through the center line of the outer shroud. This is shown in Figure 3. The general formulation for the gap of crevice is

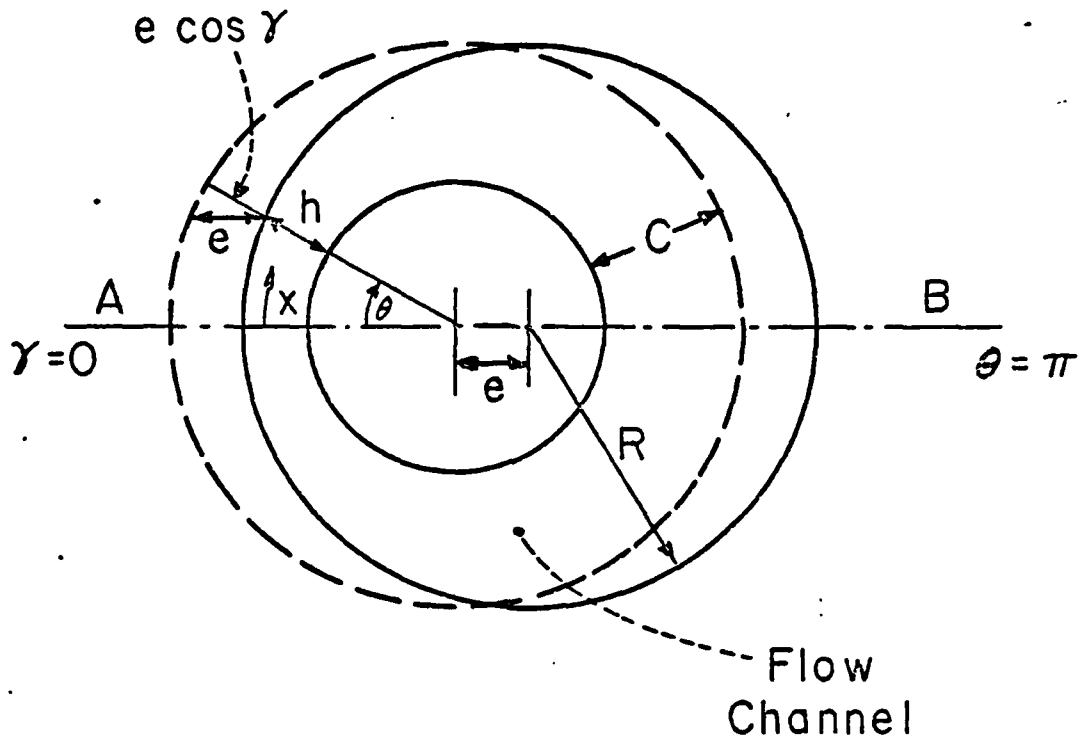

$$h\ (\theta) = C\,(1 - \epsilon \cos\theta)$$

Fig. 2. The Bottom View of Eccentric Annulus

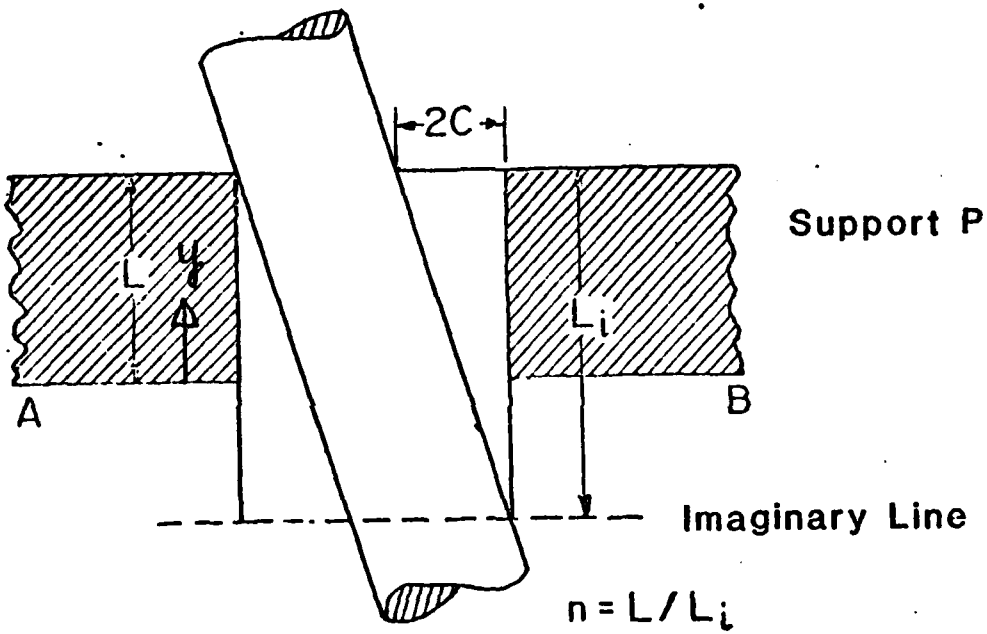

$$\delta(x,y) = C\left\{1-\epsilon\left[1-2n\left(1-\frac{y}{L}\right)\right]\cos\gamma\right\}$$

Fig. 3. The side view of an inclined tube in support-plate hole.

$$h = c\{1-\epsilon[1 - 2n(1-(y/L))] \cos \theta\} \quad (3)$$

where the eccentricity ratio ϵ is the value at the cross-section where y= L. The n, called the index of inclination, controls the angle of inclination of the inner tube. When n equals zero the inner tube is in parallel with the outer shroud. At this moment the equation (3) is the same as equation (2). When the n increases but with the ϵ fixed, the angle of inclination of the tube increases while its relative position at y = L is not changed. When n equals unity, the inner tube inclines symmetrically in the crevice from a side view. For the extreme condition of ϵ = 1 and n = 1, the inner tube contacts the outer shroud at two points y = 0 and y = L respectively.

The cross-sectional view of the crevice, as shown in Figure 2, is symmetric with respect to the line A-B. Therefore, only half of the total crevice has to be calculated. In the present study the gap thickness h is generally much smaller than the tube radius R such that the curvature of the crevice can be neglected. Therefore, the crevice can be analyzed as a flattened channel with the varying height h as shown schematically in Figure 4. The dimension of the flat channel is L in the y direction and πR in the x direction with a local height h(xy). The symmetry conditions will be applied to the lines of x = 0, and x = πR.

FORMULATION

Viewing the flow field from the x-, lane as many individual flow subchannels along the y-axis, the conservation equations can be formulated for each node of each subchannel. A schematic of the divided subchannels and nodes is shown in Figure 5. compared with conventional differential analysis, the present approach allows for more simplifications for an efficient calculation yet with reasonable accuracy. Due to the simplicity, the subchannel analysis is able to calculate the complicated two phase convective boiling with minimal extra effort.

In the analysis, calculation is performed two-dimensionally on the x-y plane with a variable gap thickness h. The velocity and the temperature appearing in the analysis are the averaged value and the bulk mean value respectively over the thickness h. It is assumed that the axial pressure gradient is identical on all the nodes which are at a same axial elevation [4]. This assumption is reasonable because the magnitude of the cross flow is usually smaller than the axial flow. In the two phase region, the fluid is assumed to be homogeneous with no slip between the phases.

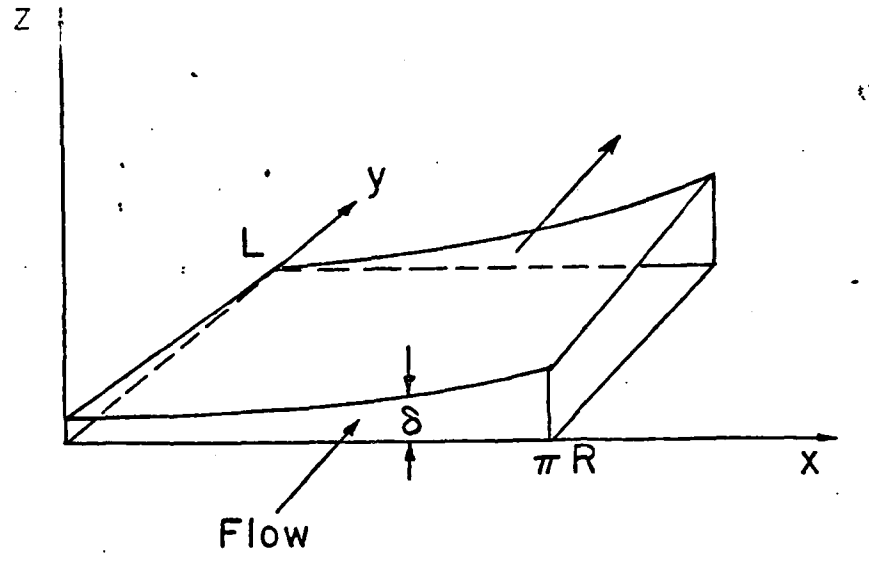

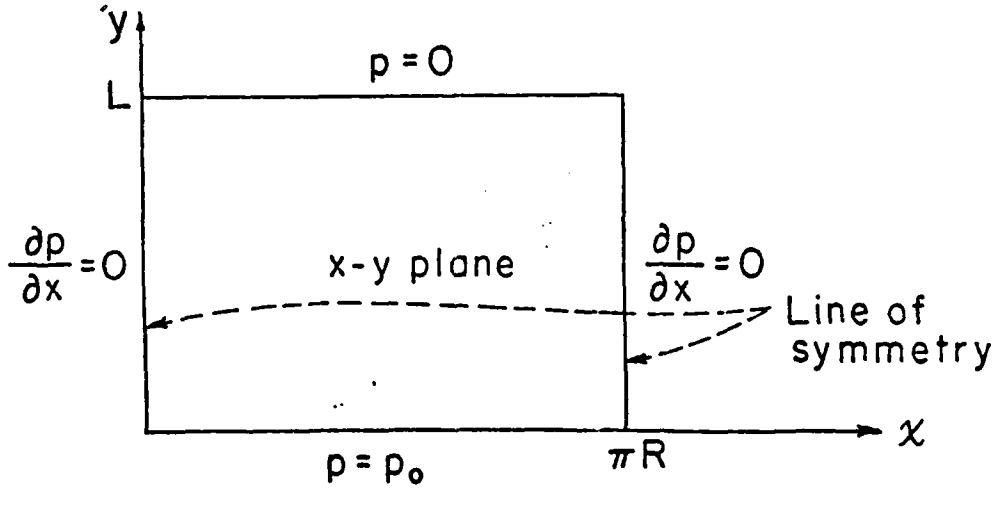

Fig. 4. Typical Geometry of the Crevice Considered in Analysis

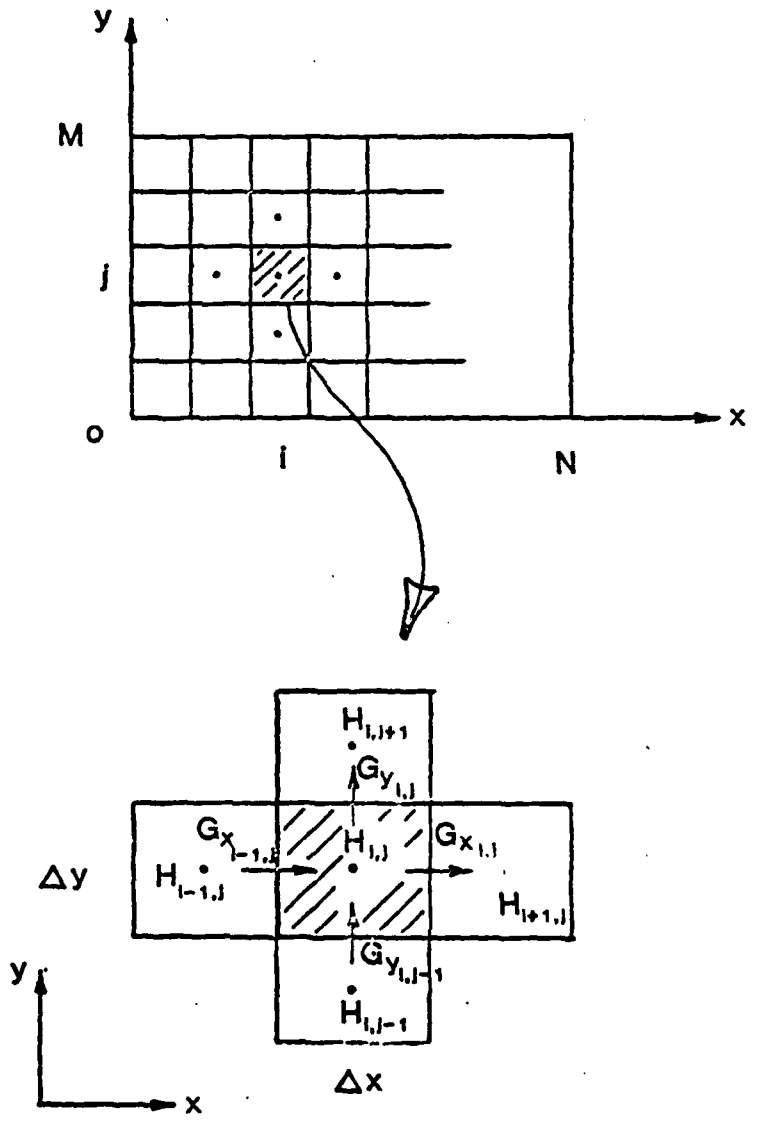

Fig. 5. The control volume in subchannel analysis.

Flow Field

Two phase flow is analyzed in the confined space. The surface tension effect at the interface is neglected. It is true that the gap thickness is extremely small near the location of contact such tnat the surface tension effect σ/h would be significant there. However, it is also likely that dryout may occur mostly at the contact area. Therefore the dryout interface would be at the location away from the surface tension dominated area except at the upstream front of the dryout zone.

At steady two phase flow the pressure force is balanced by the frictional force and the acceleration force. The gravitational effect is neglected. As will be discussed later, generally the flow stream passes along the dryout boundary such that the change of flow quality is not very severe. Therefore the acceleration pressure drop is negligible compared with the frictional pressure drop which is rather significant in the narrow space. The pressure force is balanced by the frictional force. That means

$$-\left(\frac{\Delta p}{\Delta y}\right) = \Phi \frac{f_\ell}{D_h} \frac{1}{2} \frac{G_y^2}{\rho_1} \tag{4}$$

where the f_ℓ is the friction factor for liquid flow with the same mass flow rate as the two phase mixture the value of 96/Re is used for laminar flow, D_h is the local hydraulic diameter which equals 2h, Gy is the local axial mass flux, and Φ is the two phase friction multiplier. For homogeneous non-slip two phase flow, the friction multiplier may be described as [5]

$$\Phi = 1.0 \quad \text{when } \beta < 0 \tag{5}$$

$$= \left(\frac{\rho_1}{\rho}\right) \quad \text{when } \beta > 0 \tag{6}$$

where β is the local quality of the fluid, ρ is the local density of the homogeneous two phase fluid.

At a specific elevation, the local axial mass flux $G_{y_{i,j}}$ in the subchannel (i,j) can be evaluated from equation (4). The total axial mass flow rate in the crevice is the summation of all the axial flow rates over all the i subchannels

$$\dot{m} = \sum_{i} G_{y_{i,j}} h_{i,j} \Delta x \tag{7}$$

Substituting equation (4) into (7), the total axial mass flow becomes

$$\dot{m} = \sum_{i=1}^{n} \left[\frac{2\rho_l \cdot D_{hi,j}}{\phi_{i,j} f_{\ell i,j}}\right]^{1/2} \left[\left(-\frac{\Delta p}{\Delta y}\right)_{i,j}\right]^{1/2} h_{i,j} \Delta x \tag{8}$$

Once the axial flows are determined, the local cross flows can be evaluated from the mass conservation at a node. As shown in Figure 5, the mass conservation gives

$$Gx_{i,j} h_{i+1,j} \Delta y = Gx_{i-1,j} \Delta y \tag{9}$$
$$+ Gy_{i,j-1} h_{i,j-1} \Delta x - Gy_{i,j} h_{i,j+1} \Delta x$$

where the G_s and $Gy_{i,j}$ are known from the axial flow calculations. the boundary condition of symmetry at x = 0 gives

$$Gx_{i-1,j} = 0 \text{ at } i = 1 \tag{10}$$

All the other cross flows can therefore be evaluated.

Thermal Field

The enthalpy balance in the control volume of a node can be made according to Figure 5 as

$$Gy_{i,j-1} h_{i,j-1} \Delta x \, H_{i,j-1} + Gx_{i-1,j} h_{i-1,j} \Delta y H_{i-1,j} \tag{11}$$
$$+ q_w \Delta x \Delta y = Gx_{i,j} h_{i+1,j} \Delta y H_{i,j}$$
$$+ Gy_{i,j} h_{i,j+1} \Delta x \, H_{i,j}$$

where G is the local mass flux, H is the local enthalpy, and q_w is the local heat flux from the wall. The signs used in equation (11) are based upon the flow directions indicated in Figure 5. When cross flow is different from those assumed in Figure 5 the form of energy balance equation will be modified accordingly.

For a steam generator the wall heat flux can be evaluated as

$$q_w = (T_t - T)/\left(\frac{1}{h_t} + \frac{\delta}{k_t} + \frac{1}{h_s}\right) \quad (12)$$

where h is the heat transfer coefficient, δ is the tube wall thickness, and the subscripts t and s are for the tube side and the shell side in crevice respectively.

Once the local enthalpy is known the local flow quality can be evaluted from

$$H = H_{lsat} + \beta H_{fg} \quad \text{for } 0 < \beta < 1 \quad (13)$$

NUMERICAL METHOD

A computer program has been established to perform the above calculations. The fluid flow in a crevice is driven by a given pressure difference cross the support-plate. Iteration of the mass flow in the crevice is necessary to match this given pressure drop.

Initially, the local quality β and the total mass flow m are assumed. Then calculation is performed on the nodes at a same y elevation. The local friction multiplier $\Phi_{i,j}$ is evaluated from the assumed local quality and fluid properties using equation (6). Using an assumed local friction factor $f_{i,j}$, the local pressure gradient $(-\Delta p/\Delta y)_{i,j}$ at this y elevation is calculated from equation (8). Iteration of equation (8) is necessary to obtain the converged $f_{i,j}$'s. Then the nodes at the next y elevation are calculated in a similar manner to evaluate the local pressure gradient at this new elevation. After calculation of the whole flow field, individual pressure drops at each elevation are summed to check against the given pressure difference across the support-plate. Through comparison, the initially assumed total mass flow rate m is updated. This iteration continues until the total mass flow rate matches the given pressure difference across the support-plate.

The next step is to evaluate the local cross flow from equation (9). Then the local enthalpy is calculated from equation (11); and the local flow quality is obtained using equation (13). With the up-dated local fluid quality x at every node the overall calculation of flow and energy is repeated until all the local qualities converge.

In the computation, numerical instability has been observed. When the initial guess of local quality is very much away from reality, the change of local cross flow between iterations could be significant. The variation of local qualities in iterations also becomes large. Due to the highly sensitive response of Φ to changes in quality

or fluid density, numerical instability occurs. The simpliest way of suppressing the instability is to under-relax [6] the coupling term during the iteration between the energy equation and the motion equation. This technique is found to be effective.

In the numerical calculations, the typical mesh is about 18 nodes in x domain to cover 180 degrees, and 20 nodes in y direction to cover the length of the crevice. To allow the flow quality to converge between the motion and the energy equations about 30 iterations are required. The complete calculation of boiling and dryout patterns uses about 24 seconds of cpu time on a DEC-20 computer.

RESULTS AND DISCUSSION

The boiling and dryout in the crevice at line-contact is calculated [7] for data conditions similar to those reported in reference [1]. In that experiment, pressurized water containing impurities flows through the crevice for a long duration of time. The liquid in the tube is at a higher temperature under forced convection. Boiling occurs at the location where the tube contacts the wall of the support-plate hole. Due to the excessive boiling and dryout, solid impurities deposit at the boundary of the dryout zone. The experimental condition which has been used as the input information of our calculation is listed in Table 1.

Table 1: INPUT INFORMATION FOR THE COMPARISON OF CALCULATION AND DATA [1]

Tube	I.D.	1.905	cm
	Thickness	1.092	mm
	Material	Inconel-600	
Support-Plate	Hole Diameter	1.9634	cm
	Height	1.905	cm
Shell-Side	Water,Pressure	5.442	MPa
	Inlet Quality	0.15	
	Pressure Drop	2.04	KPa
Tube-Side	Water	588	K

The calculated result and the experimental data are compared in Figure 6. The result of one-dimensional analysis performed in reference [1] is also shown in the figure. The result of the present calculation is similar to the result of the one-dimensional calculation, and both results are reasonably close to the experimental data. This is mainly because the crevice with a line-contact configuration does not

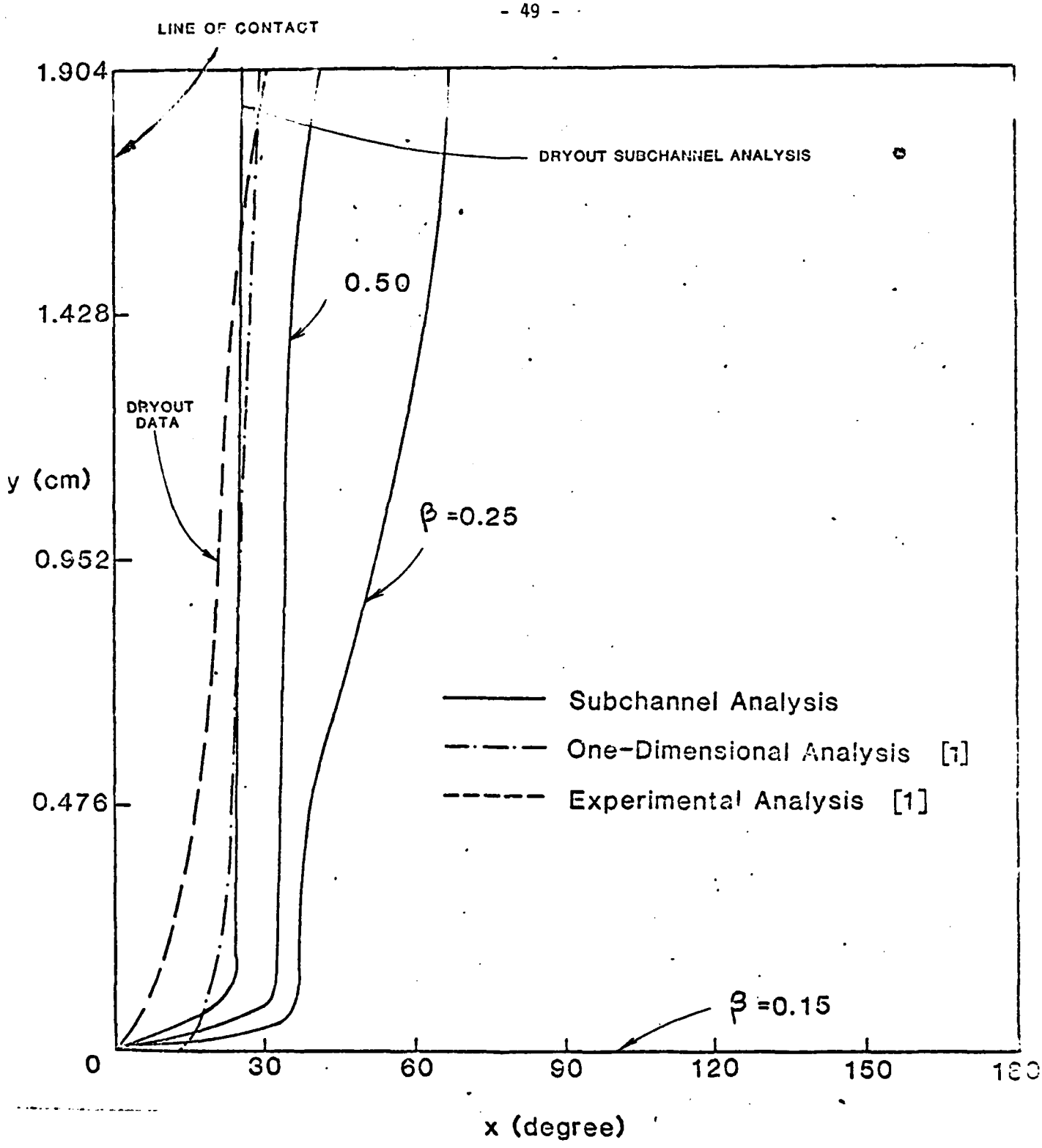

Fig. 6 The patterns of dryout and flow quality of line-contact configuration.

have a sizable cross flow. (The tube is in parallel with the hole axis). Therefore the difference between the present analysis and the one-dimensional analysis is not obvious.

The behavior of dryout is also studied for the condition of one-point- contact but at various inclinations. As shown in Figure 7 the contact point is at the top of the clearance at zero degree. With more and more inclination (as denoted by higher value of n) the dryout zone becomes less and less. At the extreme condition of n = 1.0 when the tube contacts the shroud at two points (at the top of zero degree and the bottom of 180 degree) another dryout zone also appears at the location near 180 degrees with significant effects to its downstream. From this general observation it becomes clear that both the configuration of line-contact and two-point-contact induce dryout over a large area. However, limited dryout occurs for the configuration of one-point-contact.

In practical heat transfer devices it is difficult to avoid or to control the way of contact between the tube and the support plate. But it is possible to drill the hole on support plate with a special configuration, for example, a square hole that the contact occurs between the tube and the support-plate but with a large opening for flow by-pass. To understand the dryout at this condition, calculations are performed for the geometry of line-contact but with various averaged-gap-thickness of the annulus, c. As shown in Figure 2 the larger the value of c the more the difference of the radii of curvatures near the contact location. The calculated results are shown in Figure 8 which indicates that the larger the difference of the radii of curvatures the less the dryout zone. In the present study, when c is larger than 2.117 mm the dryout zone will disappear completely. In fact, the similar conclusion has been obtained from the experimental studies reported in the reference [1]. A very good confirmation between the present analysis and the experimental results in [1] suggests that this computation method can be used as an effective tool for better design of steam generator support-plates to minimize or avoid the dryout, induced corrosion.

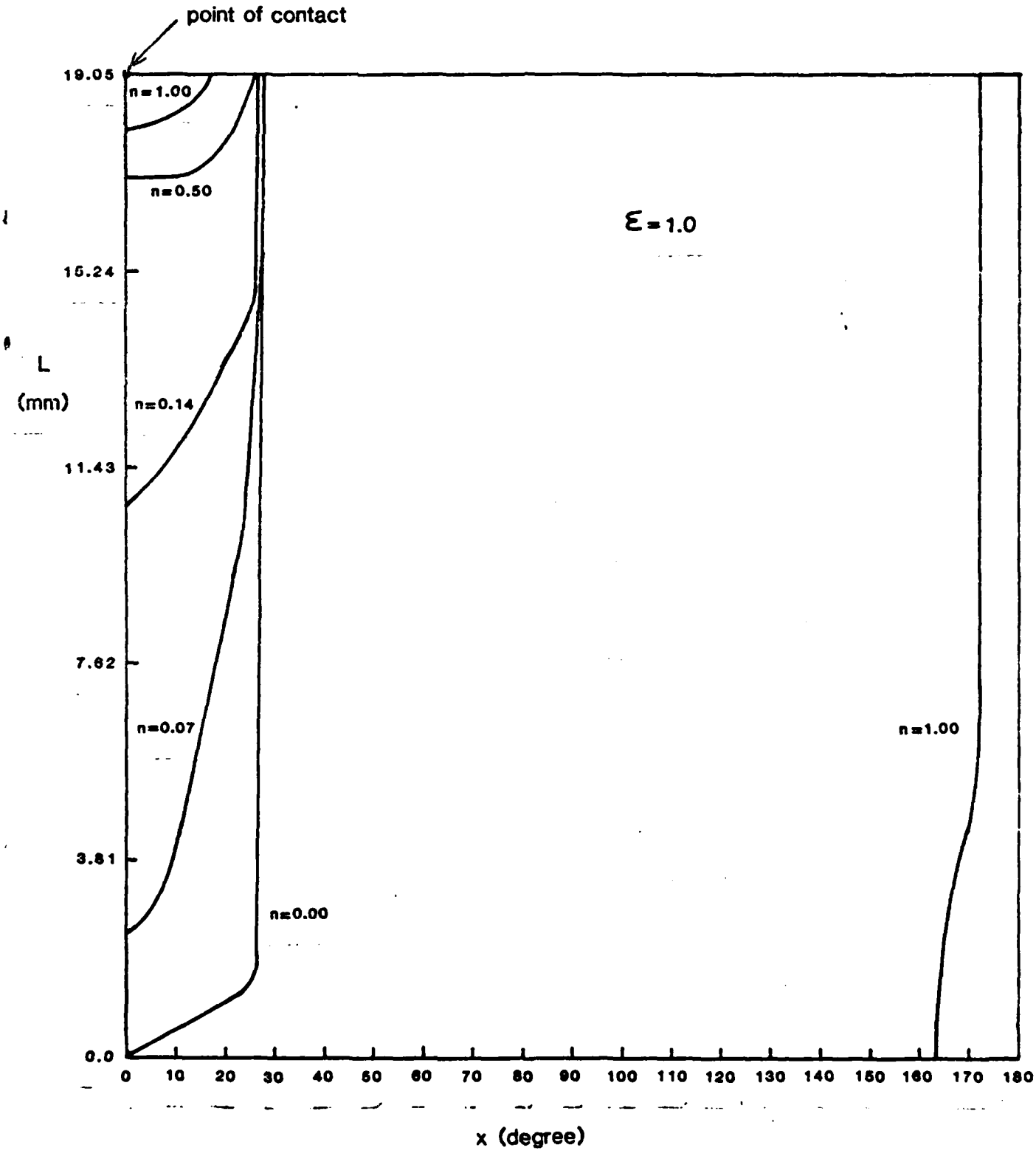

Fig 7. The calculated dryout pattern in annular clearances with inclined tube and contact at one-point.

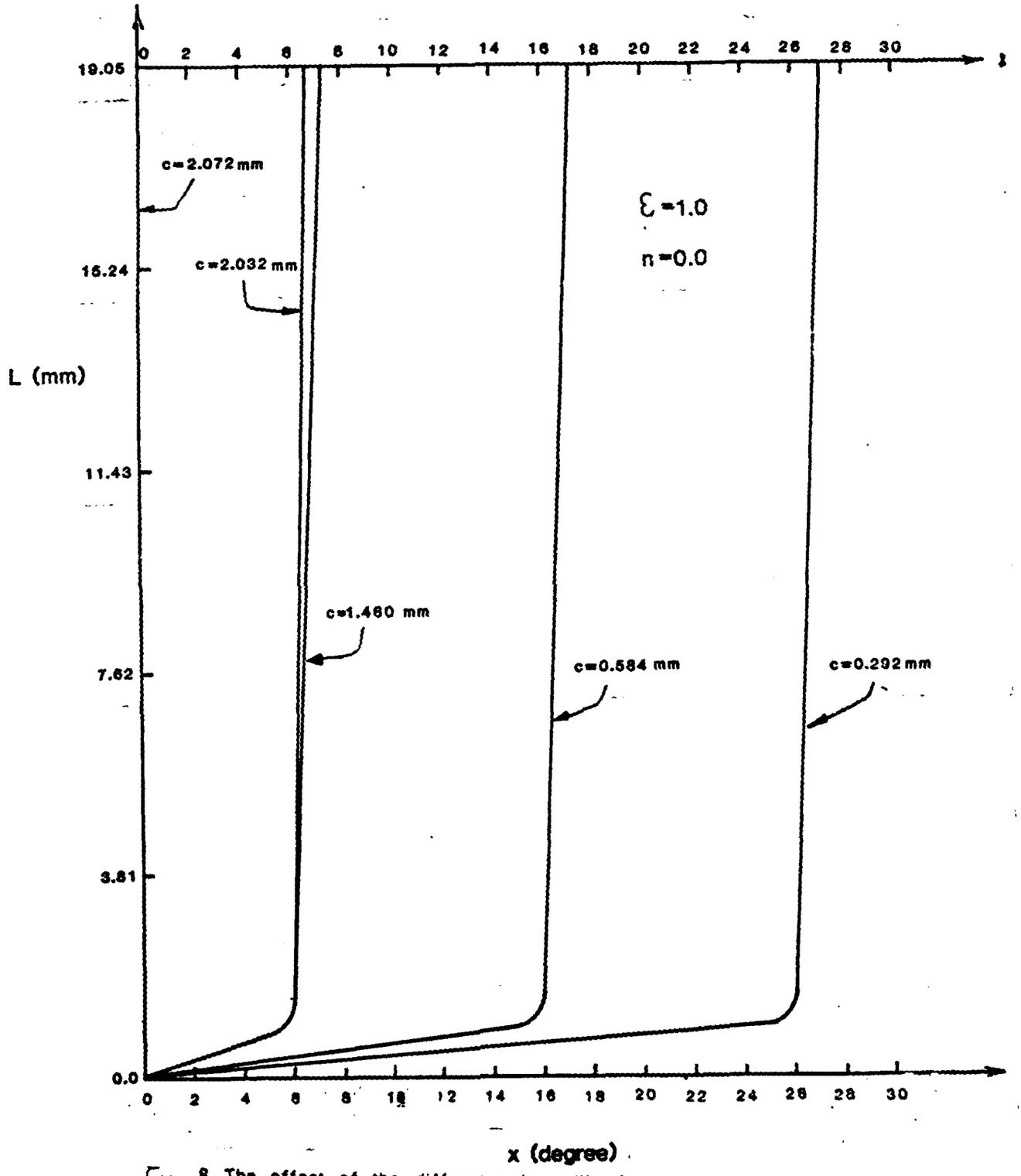

Fig. 8. The effect of the difference in radii of curvatures near the line-contact area to the dryout pattern.

CONCLUSION

The present subchannel analysis gives reasonable prediction of boiling and dryout in confined space at forced convection. For heated tube passing through round holes on support-plate with small clearances, the dryout always occurs near the location of contact. When the difference in radii of curvature increases, the dryout zone decreases and finally disappears. Utilizing this particular feature which is predicted in the present analysis, better design of the support-plate can be achieved.

REFERENCES

[1] Baum, A.J., and Curlee Jr. N.J., "An Experimental and Analytical Investigation of Dryout and Chemical Concentration in Confined Geometries," ASME Nuclear Eng. Division Conference, San Francisco, August 18-21, 1980.

[2] Rowe, D.S., "Cross-Flow Mixing Between Parallel Flow Channels During Boiling Part I, COBRA-Computer Program for Coolout Boiling in Rod Arrays," BNWL-371, PT1, 1967.

[3] Sha, W.T., and Schmidt, R.C., "THI-3D A Computer Program for Steady-State Thermal-Hydraulic Multichannel Analysis," ANL-8112, 1975.

[4] Jones, O.C., Yao, S.C., and Henry, R.E., "SIMPLE-2, A Computer Code for Calculation of Steady-State Thermal Behavior of Rod Bundles with Flow Sweeping," Nuclear Engineering and Design, Vol.41, pp.205-217, 1977.

[5] Collier, J., Convective Boiling and Condensation, McGraw-Hill, 1972.

[6] Patankar, S.V., Numerical Heat Transfer and Fluid Flow, McGraw-Hill, 1980.

[7] Yao, S.C., "Boiling Heat Transfer in Confined Space," Carnegie-Mellon University Report No. 00014-79-C-0623-1980A, 1980.

CHAPTER 4

EXPERIMENTS OF BOILING AND DRYOUT IN ANNULAR CREVICES WITH CLOSED BOTTOM

INTRODUCTION

I. Literature Review

Katto and Yokoga et. al [1] [2] [3] [4] investigated confined space boiling of saturated water on a horizontal flat plate. A movable optical assembly was placed above a heated surface and had a small gap in between. The boiling in the narrow gap has higher heat transfer coefficient which is due to the existence of thin liquid film under bubbles . They suggested that the dryout condition in confined space is a balance between the consumption of the liquid on the heated surfac and the supplying of the liquid between the intermittent jetting of vapor mass.

Ishibashi and Nishkawa [5] conducted the boiling experiment for vertical annulus with open ends. It was determined that there are two distinct boiling regimes, each having different heat transfer characteristics. No quantitative information for dryout had been obtained.

The experiment of boiling of an horizontal tube within constrain was conducted by Jensen, Cooper & Bergers [6]. The increase in the heat transfer was also explained by the thin film evaporation. The dryout heat flux was found to be directly proportional to the clearance and inversely proportional to the length of annulus. Compared to a open tube, the dryout heat flux was reduced by a factor of 10.

Kusuda and Imura [7], [8] performed experiments with subcooled and saturated liquid for boiling heat transfer in vertical closed bottom tubes and annuli. The annuli experiments consisted of an unheated core and an externally heated tube. The heat transfer coefficient of boiling was reported to be independent of the length and the diameter of the heated tube. The correlation for dryout heat flux was attempted by dryout analysis but it was not able to correlate satisfactorily with their experimental results. The visualization of boiling was done in separate tests.

2 Objective

Increased knowledge about boiling heat transfer in a closed bottom annulus will improve our understanding of thermal-hydraulic related corrosion in nuclear steam generators. The available data in the literature on saturated boiling in vertical closed bottom annulus is not sufficient for a thorough analysis.

It has been demonstrated by Ishibashi and Nishkawa [5], that in a confined space, heat transfer characteristics are closely associated with the boiling pattern in the crevice.The experiment with visualization and heat transfer measurement at the same time will give more detailed understanding of the boiling mechanism in the vertical closed bottom confined space.

With the geometric configuration shown previously, the crevice is likely to have permeanant nucleation sites at its bottom end. Therefore the experiment will be conducted in a closed-bottom vertical annulus with existing nucleation sites at its bottom. The objectives of this experimental research are as follows:

1.To investigate the effect of gap size and system pressure on saturated boiling in vertical closed-bottom annulus with existing nucleation sites.

2.To study the effect of fluid properties on the boiling heat transfer using Freon-113, acetone and distilled demineralized water.

3.To observe the boiling behavior in a confined space through movie and to propose correlations to interpret the experimental results.

Since the dryout heat flux has its practical importance, attention will be paid to the correlation of the dryout heat flux to fluid properties and geometry.

EXPERIMENTAL APPARATUS AND PROCEDURE

1 Experimental Apparatus

Experiments have been conducted by boiling of Freon-113, acetone and distilled demineralized water on the outside of an electrically heated tube which was placed inside a an hollow quartz cylinder with a small gap in between. The annulus is closed at the bottom and open at the top. The test assembly was immersed in a pool of saturated liquid as shown in Fig. 1. An enlarged view of temperature measurement device is shown in Fig. 2.

The heating tube used in all the experiments is stainless steel 304 seamless tubing 25.4mm O.D. with 0.71mm wall thickness and 101.6mm heated length. The top of heating tube was thermally shrink-fitted into a copper tube with the same outside diameter and 1.42mm wall thickness. The bottom end of the tube is fitted into a copper block. Direct current passes though the heating tube from the upper copper tube to the bottom copper block.

As shown in Fig. 3, the hollow quartz cylinders are 95.3mm long with 63.5mm O.D. The inside diameter 26.04, 27.00 to 30.58mm to form different sizes of gap with the tube. The inside diameter is enlarged at the top and bottom to accommodate the positioner. The inner and outer surfaces of quartz tube was polished to 50-80 finish and is clear enough to see through.

The three gap sizes tested are 0.32, 0.80 and 2.58mm, with all of them

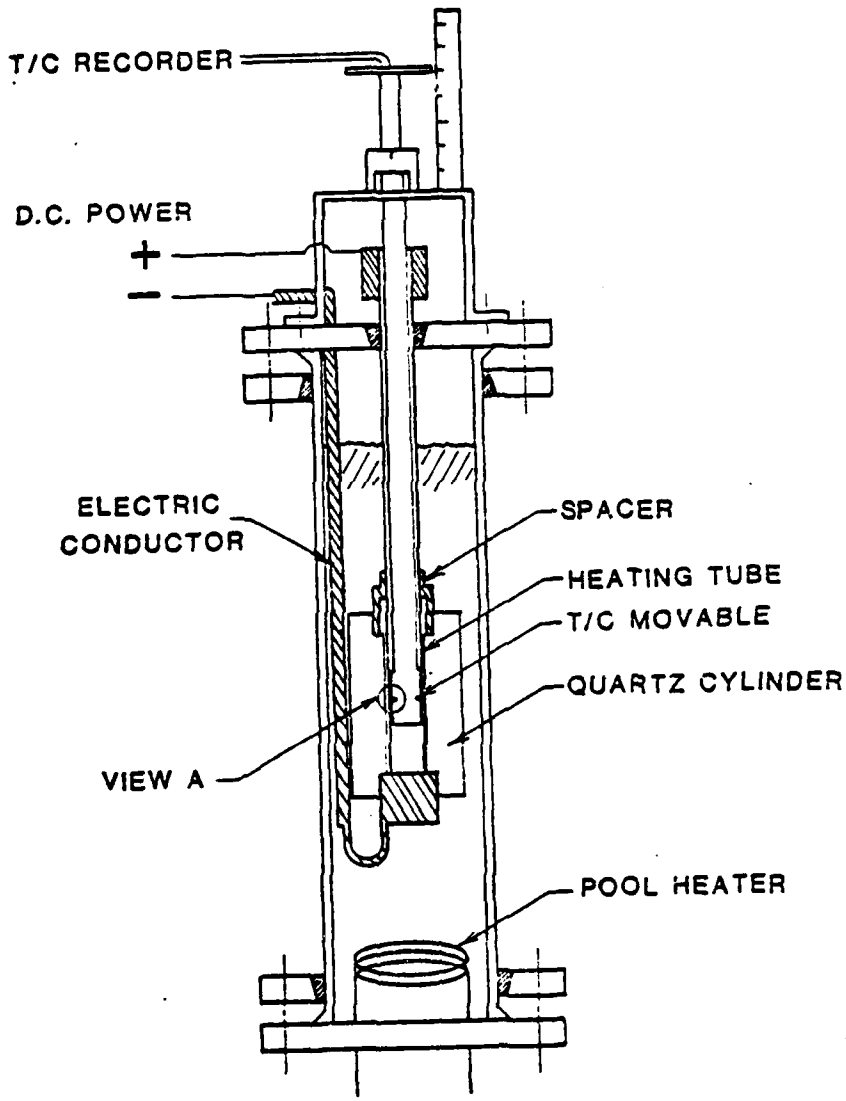

Figure 1: Confined Space Experimental Setup

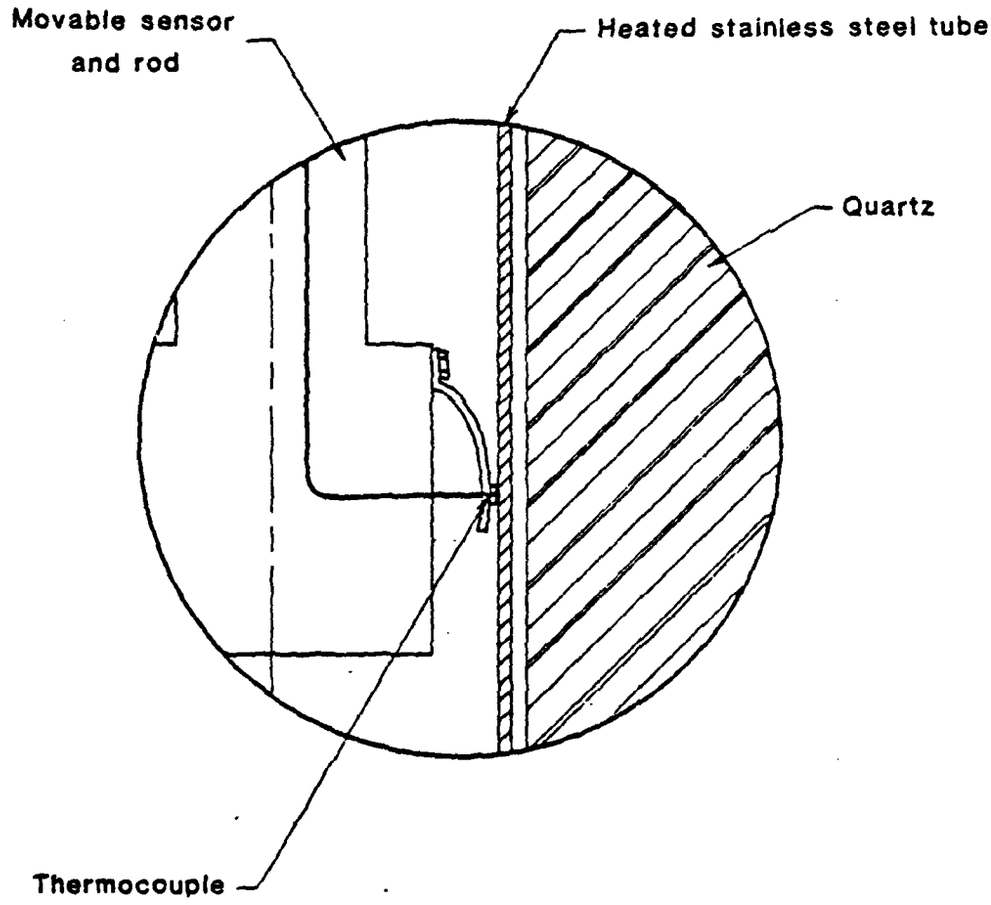

Figure 2: Enlarge View of Temperature Measurement Devices

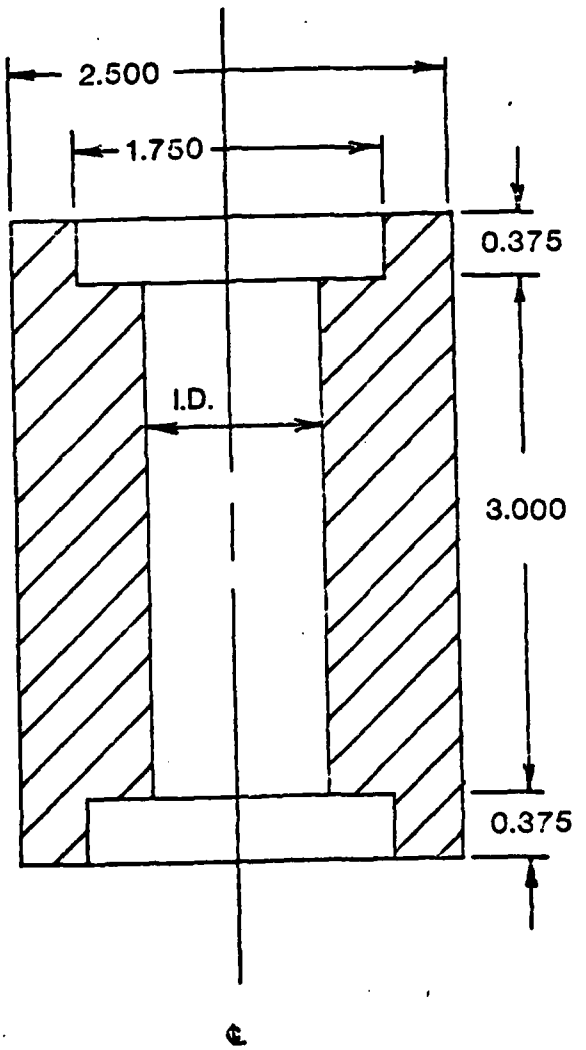

Figure 3: Detail Drawing of Hollow Quartz Cylinder

76.2mm long. There is another test section with 0.32mm gap but only 25.4mm long. To achieve a uniform gap thickness, the top and bottom positioners were installed to maintain the relative concentric position of the heating tube and the outer quartz. The bottom of the crevice was sealed by a Teflon ring which does not interact with Freon-113.

The Freon-113 pool is contained by a 101.6mm I.D. and 457.5mm length Pyrex glass pipe. The pipe is closed at both ends by flanges with Teflon seal, with beaded end. The allowable operation pressure is 4.4atm. A 12.7mm I.D. tubing was connected to the top of the tank to release the Freon vapor generated by boiling. The vapor was then condensed in a water cooled condenser. The consumed Freon-113 liquid was refilled from the bottom of tank by siphon from an outside reservoir. The saturation temperature of the pool was maintained by an immersion heater, which was adjusted by a Variac. A type k ungrounded thermocouple was installed in the pool to measure its temperature, and the system pressure was monitored by a pressure gauge. For pressurized tests a compressed nitrogen cylinder was connected to supply the pressure. For low pressure tests a diffusion vacuum pump was used.

The electric current passing through test section was measured by the voltage drop across a calibrated shunt using a Hewlett-Packard 3465S digital multi-meter. The power was provided by two direct current welders. A Miller Direct Current Arc Welder supplies the current in the range of 20-300 amps. A Westinghouse WSH Arc Power Supply Direct Current supplies current between 200-1000 amps. The current was conducted to the test section through a 25.4mm O.D. copper cable which was clamped to the connectors of test section. A supporting structure was built to support the weight of cables.

Inside the heating tube, the temperatures can be measured at different locations. Two type k stainless sheathed miniature thermocouples with the

0.81mm diameter were pressed against the inner wall by springs with a force of 0.48 newtons. The springs and thermocouples were mounted on a micarta cylindrical body which blocked the tube to avoid natural convection. The thermocouple was calibrated within the setup by immersing the heating tube in constant temperature open pool. The pool temperatures were determined by maintaining different liquids at their saturation temperatures. The thermocouples were connected to OMEGA Trendicator. The displayed temperature has an accuracy of ±0.56 °C.

2 Experimental Procedure

The same heating tube was used for all the tests. The surface was polished before each test with a #320 sandpaper to remove any print, soot, flux or other surface irregularities so that a consistent surface finish would be obtains for all tests.

The liquid level was maintained nearly constant at 100 mm above the top of the crevice during the test by periodically adding make-up liquid to the pool. If the liquid is only slightly above the heating tube, violent boiling could uncover the tube and caused premature dryout. The test section is preheated by a heat flux of 21 kw/m^2 and preboiled for at least one hour. For water tests with the smallest gap size, gas bubbles may be trapped inside the annulus . The preheating for water test required much longer time then the other liquids to remove these entrapped air bubbles.

The nucleation site at the bottom of crevice is formed naturally between the Teflon seal and the copper block. In steam generator the crevices at the bottom of the tube sheet may contain permeanent nucleation sites. Therefore the test is performed with the nucleation sites at the bottom of crevices.

The steady-state data was taken 3 minutes after the change of heat flux. The thermocouples are located 1.2cm below the top opening of quartz in order to detect the early dryout.The movie was taken with a Borax movie camera at the speed of 64 frames per second with top lighting. Kodak 4712 Tungsten light balanced color film was used.

The location of thermocouple could be changed during the test to check the axial variation of wall temperature. The wall heat flux was calculated from the measured eletric current and the known electric resistance of the stainless steel tube. The inner wall temperature was measured by thermocouple. With known inside temperature the outer surface temperature was calculated from the steady-state heat conduction equation in cylindrical coordinates, with one-dimensional heat flow and constant physical properties.

RESULTS AND DISCUSSIONS

1 The Boiling Heat Transfer of Freon-113

Both the confined space and open pool experiments was conducted in the Freon-113 pool. The results are discussed in the following sections.

1.1 Boiling in the Open Pool

The tests were done in the Freon-113 pool without the quartz cylinder at its outside. The heat is transferred by natural convection until boiling occurs.

1. Natural convection: At low heat flux, natural convection is the dominant heat transfer mode. The natural convective heat transfer for a vertical cylinder with large Prantdl number is reported by Eckert [9] as

$$Nu_x = 0.508\ (Pr/(0.92+Pr)*Gr_x Pr)^{1/4}$$

where the x is the distance measured from the bottom of tube. The experimental data are compared with this equation in Fig.4 . The error is within 10%.

2. Pool boiling:

At a higher heat flux, bubbles are generated on the heating surface. The heat flux increases drastically with the wall temperature. In this experiment the relationship between the heat flux and wall temperature super heat is in the form of

$q \propto \Delta T^3$

The data of present F-113 experiments are plotted in Fig.(ref.(pool boiling)) . Also included in the same Figure is the experimental data of Yilmaz and Westwater [10]for a horizontal copper tube (20 gauge, 6.4mm O.D.) heated by steam. The curves of these two experiments are parallel although they are in different orientation with respect to gravity. It is important to point out that the open pool results of present experiment does not reach the critical heat flux.

The data of another F-113 experiment by Hesse [11] also plotted in the Fig. 4 . The tube is made of nickel with 14mm O.D. and heated by hot water situated horizontally in the pool. The boiling curve is to some extent different from the result of present study and the data of Yilmaz and Westwater. The discrepency may due to the different liquid-solid combination and orientation of the heater.

1.2 Boiling in the Confined Space

The boiling of F-113 in confined space has been studied with the gap sizes of 0.32, 0.80 and 2.58mm. The effect of different lengths and operating pressures are also studied for the smallest gap size. The test conditions are as listed in Table 1.

Table 1. Summary of F-113 Experiments

Test Sections	Gap (mm)	Length (mm)	Pressure (atm)
1	0.32	25.4	1
2	0.32	76.2	0.6,1,2.02 3.04,4.4
3	0.80	76.2	1

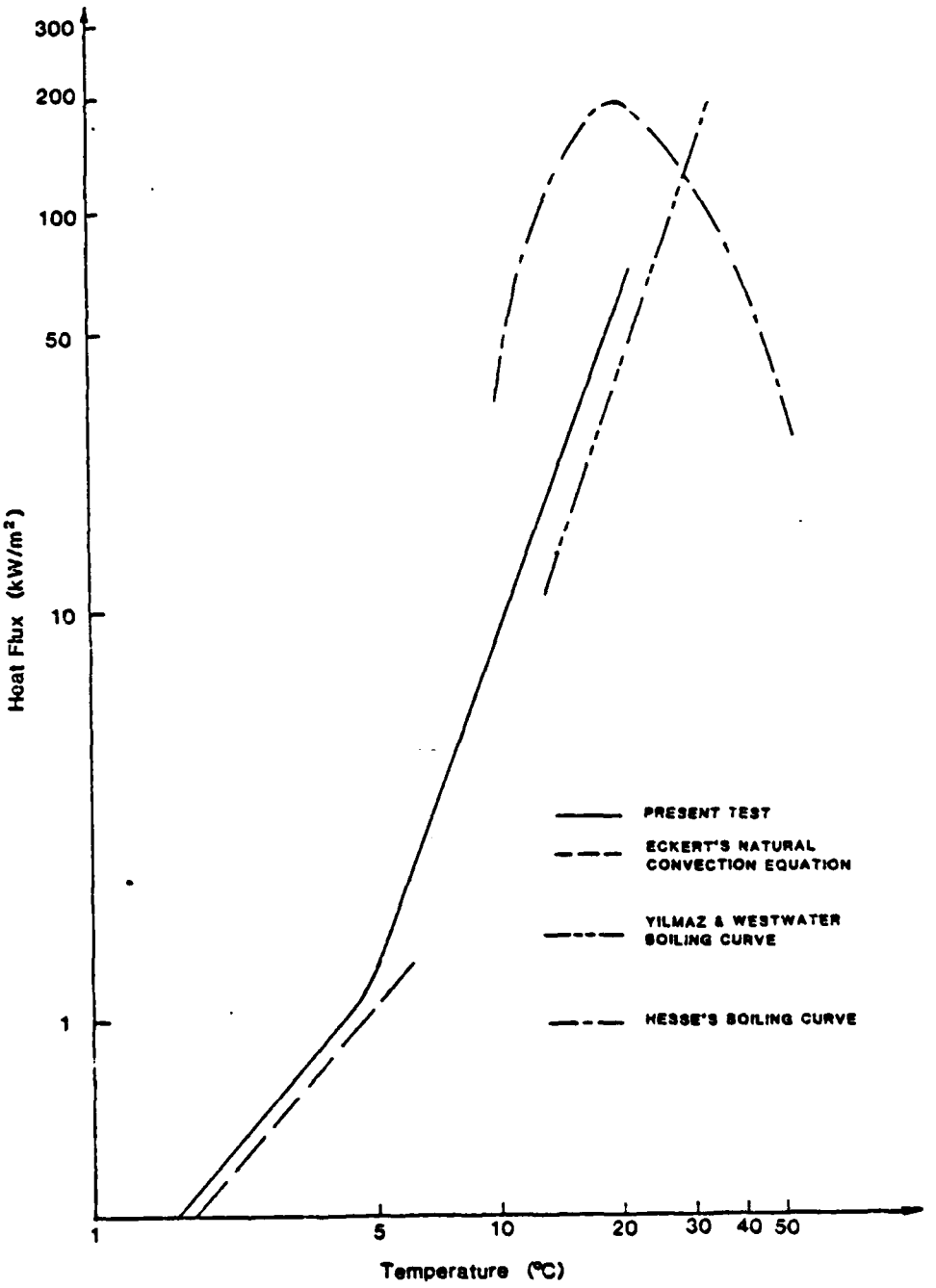

Figure 4 Open pool boiling Curve

4	2.58	76.2	1
open pool	-	101.6	1

Boiling in the confined space has been closely observed in the present study. The most important feature is that bubbles are squeezed due to the small gap between the walls. The shape and motion of the bubble are seriously affected by the restricted space. In this experiment the bubbles are mostly generated from the bottom of the crevice. With the addition of heat flux the phenomenon of boiling in small gaps, go through the following stages: Fig. 5.

1. Isolated Deformed Bubbles:

At low heat flux the bubbles are relatively isolated. The shape of the bubble is generally hemispherical with a flat bottom. This is in a similar shape to the very large bubble in a open pool because the drag effect is important. A thin film of liquid is formed between the bubble and the walls. With the addition of heat,the bubble enlarges itself while moves up. At low heat flux, a small fraction of the heated area is covered by bubbles and at a higher heat flux, more area will be covered.

2. Violent Evaporation of Deformed Bubbles:

At a higher heat flux, the wall temperature super-heat starts to increase. The upward moving bubbles expand rapidly. Most of the surface area is covered by the up-flowing deformed bubbles with the liquid flowing down from the top in between the bubbles. The bubble rises with a stop and go pattern by merging or interacting with other bubbles. Temporary dryout may occur under the bubbles but liquid will soon rewet the surface. For the low temperature superheat there is no bubble nucleation on the solid surface.

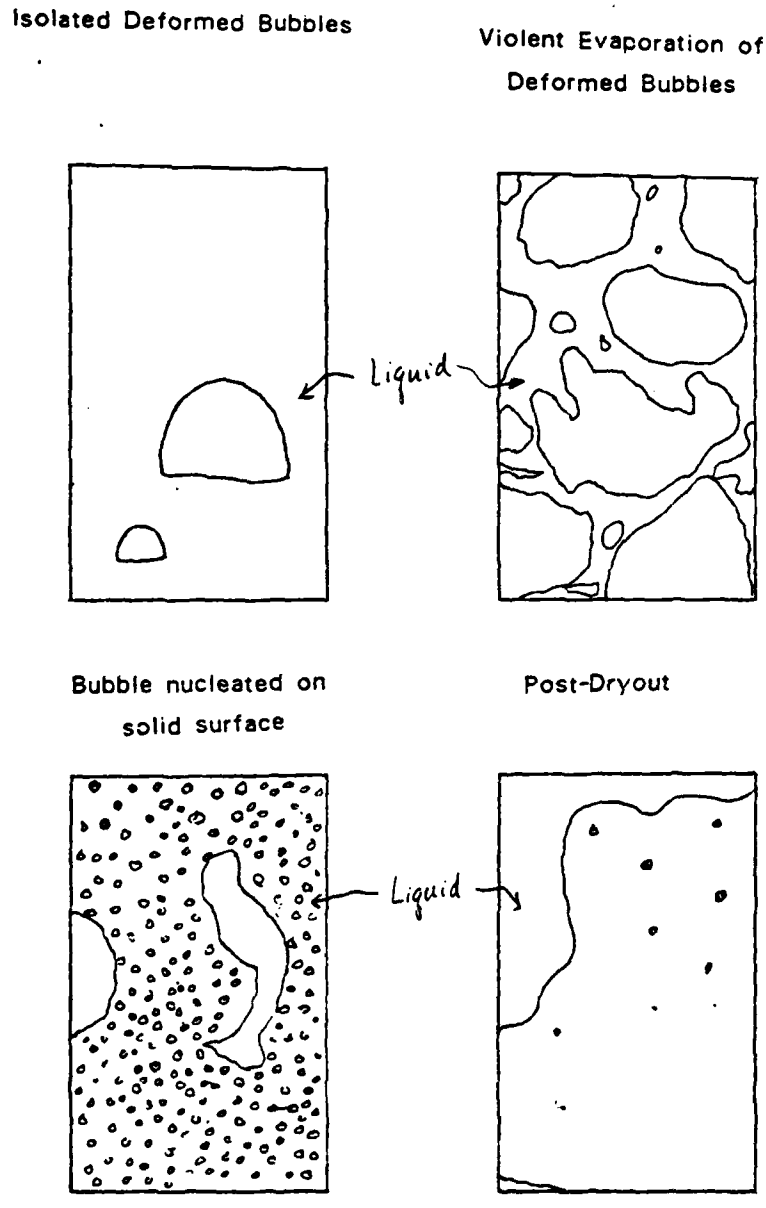

Figure 5 Boiling Phenomena in the Confined Space

3.Bubble nucleated on solid surface

If the gap is large and with a high heat flux, bubbles are generated in the thin film under the deformed bubbles. The small bubble starts at the nucleation site on the solid surface and breaks through the thin liquid film. Affected by the motion of the large deformed bubbles, the small bubble is nucleated at random location. The bubble is also generated outside the area covered by the large deformed bubbles.

4. Dryout Condition:

Dryout in this experiment is defined as the condition when the wall temperature keep increasing with time. When the heat flux is close to the dryout value, the liquid flows downward as a film at both sides of the gap the gas flows upward in between. The liquid film on the heating surface is evaporated extensively but the liquid film on the unheated quartz cylinder may extend to the bottom of crevice. The flowing film at the heated wall may dry up. However, the liquid film along the unheated wall can ,sometimes, be transferred to the heated side either by the surface wave which bridges the gap or pushed by the bubbles generated in the liquid pool which is accumulated at the bottom of crevice. Therefore the heated surface may also get cooled.

The dryout heat flux for the crevice is generally much lower than the critical heat flux of the open pool. The dryout heat flux also varies with the gap size and lengtn. It appears that the limiting criterion of dryout heat flux is no longer the same as that in pool boiling. The particular flow pattern caused by the confinement effect has to be considered as well.

5. Post-Dryout Condition:

Beyond the dryout heat flux the temperature of test section rises along the time. To avoid the burn out of the test section, the power must be shut off in a short duration of time. However, it is possible to study the post-dryout condition for crevices with very small gaps because the dryout heat fluxes of these crevices are low and, therefore, the temperature excursion rate is low.

At this condition the bulk of liquid at the top of the crevice can hardly get into the crevice. Standing waves of the interface are observed near the top of crevice. However, occasionally the wave breaks up and some drops are ejected into the crevice. The drops evaporate while descending to the bottom. At the bottom there may exist a shallow liquid slug where evaporation and boiling may occur. All the outgoing vapor provides enough flow to maintain the unstable wave at the top of crevice.

1.3 Boiling Heat Transfer

The boiling curves of Freon-113 are shown in Fig. 6. It can be seen that with the increase of the gap size the boiling curve of the confined space approaches the open pool boiling curve. Boiling in the confined space is characterized by the deformation of bubbles. The deformation of bubbles can be characterized by the ratio of gap thickness and the bubble departure diameter, which is generally known as the Bond number, which may be defined as

$$Bo = S/(\sigma/g(\rho_l-\rho_g))^{1/2}$$

The Bond number encountered in the F-113 experiments are summarized in Table 2.

Table 2 Bond Numbers in F-113 Experiments(1 atm)

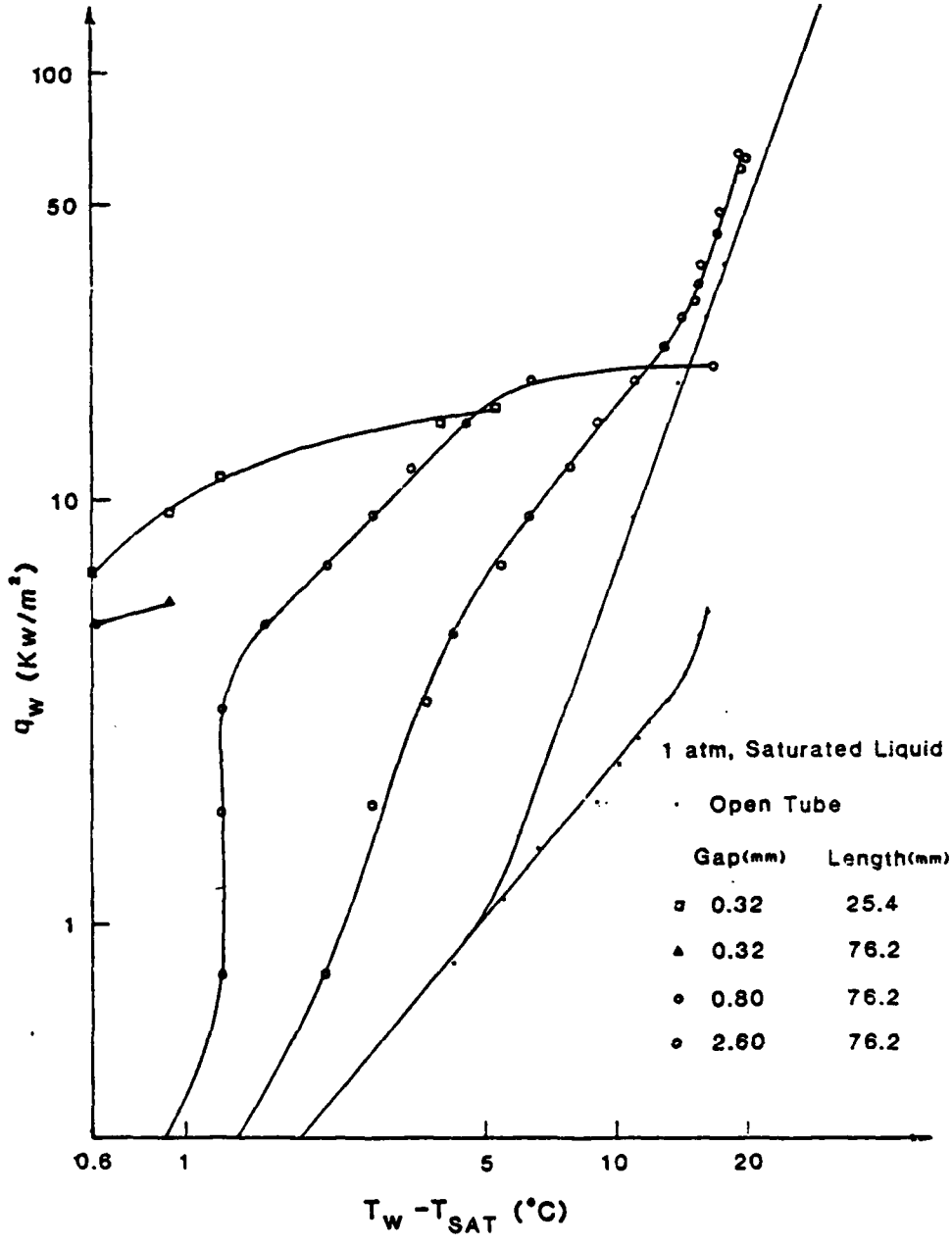

Figure 6. Boiling Curve of Freon-113 in the Closed Bottom Annulus

Gap(mm)	Bo
0.32	1.66
0.80	4.19
2.58	13.57

From the table, it is reasonable to expect that the boiling curves may differ much from the open pool results if the gap thickness is so small that the corresponding Bond number is in the order of unity. Comparing the three boiling curves in Figure 6 we may temporarily conclude that if the Bond number is small the effect of confinement would be apparent on the boiling curve. Following this, the discussion of heat transfer may be directed toward the following three different conditions and each of them correspond to a boiling phenomenoa as descibed in the last section:

(1) Large Bond Number and high heat flux.(Bubbles Nucleated on Solid Surface)

(2) Small Bond Number and low heat flux.(Isolated Deformed Bubbles)

(3) Small Bond Number and high heat flux.(Violent Evaporation of Deformed Bubbles)

The particular features of heat transfer at each condition will be discussed in turn.

(1) Large Bond Number

When the Bond Number is large the boiling curve is similar to that of the open pool. In general, the wall super heat is reduced comparing to pool boiling. At high heat flux, the boiling curve is almost in parallel to the open pool boiling curve which is in the form of

$q \propto \Delta T^3$

Chernobyl'skii and Tananaiko [12] performed experiments using water in an annulus with open ends . The dimension of the annulus was varied to give a range of Bond number from 7.9 to 31.7. They observed a similar behavior of boiling curve as indicated in Figure 6 for the large crevice which has a Bond number 13.57. They suggested that the increase of heat transfer coefficient in the narrow space is due to the reduction of the bubble size and the increase of turbulence in the mixture. The liquid is violently agitated so that a higher rate of heat removal from the heated wall occurs.

The same explanation can be applied to the case of the vertical annulus with closed bottom which was studied in this experiment.

(2) Small Bond Number and Low heat flux condition:

At this condition, the boiling phenomena is mainly isolated deformed bubbles. The heat flux increases with little increase of wall temperature. The wall temperature super heat is in the order of 0.56± °C.

The temperature super heat of bubble can be calculated follow the procedure of Griffith and Wallis ref. [13]. A small pressure difference is required to enable the bubble to exist in liquid. The Clausius-Clapeyron equation is used to calculate the bubble super heat from the pressure difference. In this experiment bubble is flattened with a radius of curvature approximately half of the gap size. The bubble super heat becomes as

$$\Delta T = 2T_{sat}\sigma / H_{fg}\rho_v S$$

The calculated superheated temperature of a flat F-113 bubble is 0.005° C

Therefore the low superheated temperature in the deformed bubble is possible.

In this low heat flux the deformed bubble only covers certain percentage of heated area.If all the heat is used to evaporate the liquid into the bubble ,the total heat flux should equal to the heat flux under the deformed bubble but corrected by the time-averaged area ratio (Ar) of deformed bubbles on heated surface.

$$q_w = Arq_b$$

The heat flux under a deformed bubble can be evaluated by the increases of bubble size over a period of time. Assuming all the heat transfer under the bubble is used to evaporate the liquid, the heat flux under the deformed bubble can be shown as

$$q_b = \Delta V \rho_v H_{fg} / A \Delta t$$

The heat flux under the bubble, the velocity of bubble and the area ratio are summarized in Table 3.

Table 3. Summary of Results from Visual observation

Total Heat Flux q (kw/m^2)	Time Interval between Successive Figures Δt (sec.)	Time Averaged Area Ratio Ar	Heat Flux under Bubble q_b (kw/m^2)
0.62	0.09	32%	2.88
0.62	0.03	32%	0.81
0.62	0.125	32%	1.33
0.62	0.125	32%	-
0.21	0.16	16%	1.29
0.21	0.125	16%	1.41

0.21	0.125	16%	-

The total heat flux equals to the thin film evaporative heat flux times the area ratio covered by the thin film. With the area ratio and the average heat flux measured from figures the total heat flux calculated are 0.54 kw/m^2 and 0.22 kw/m^2 which compared with 0.62 kw/m^2 and 0.21 kw/m^2 obtained from electric power the error is within ±13%.

From the experimental data it can be concluded that most of the heat is used in the evaporation of the deformed bubbles. The variation of the total heat flux changes the area covered by deformed bubbles,but not changing the wall superheat temperature. The boiling curve becomes almost a vertical line on the heat flux versus wall temperature . That is what we observed on the *boiling curve,(Fig. 6)under the condition of small* Bond number and low heat flux.

3) Small Bond Number and High heat flux:

At this condition most of the heated surface is covered by deformed bubbles. Unstable dryout under bubble is observed in high heat flux. The wall temperature increases with the increase of heat flux. The relationship is direct proportional

$q \propto \Delta T$

At a fixed wall temperature the heat flux is higher with smaller gap size. If the Bond number is smaller than 1.84, this region may not be observed easily.

At high heat flux the coalition of bubble occurs frequently. Eventually a center vapor core is formed with wavy liquid film flowing down on both side.

2 Boiling Heat transfer of Acetone and Water

In additional to Freon-113, boiling in acetone and distilled demineralizd water is studied. The major effect in boiling heat transfer using different fluids is the change of physical properties. Since the Bond number appears as an important parameter in describing the heat transfer in confined space, the corresponding Bond numbers of each fluid in various crevices are listed in the Table 4.

The acetone and water experiments extend the range of the Bond number to a lower range than that involved in Freon-113 experiments. Therefore the boiling curves of acetone and water may be more in similar to a that of small crevice in Freon-113 experiments.

Table 4. Summary of Bond number of present test

Gap/liquid (mm)	F-113	Acetone	water
0.32	1.66	1.03	0.72
0.80	4.19	2.60	1.84
2.58	13.57	8.23	5.87

The boiling curves of acetone are shown in the Figure 7. For crevices with Bond number less than 8.23 the curves are similar to those of small Bond numbers in Freon-113 experiments. The boiling curve of the large gap has a Bond number 8.23 and behaves similar to F-113 large gap curve with Bo equal to 13.57 and quite different from the others.

For the water experiments all the conditions have the Bond number less or equal to 5.87. Therefore the effect of confinement would be significant. As shown in the Figure 8.

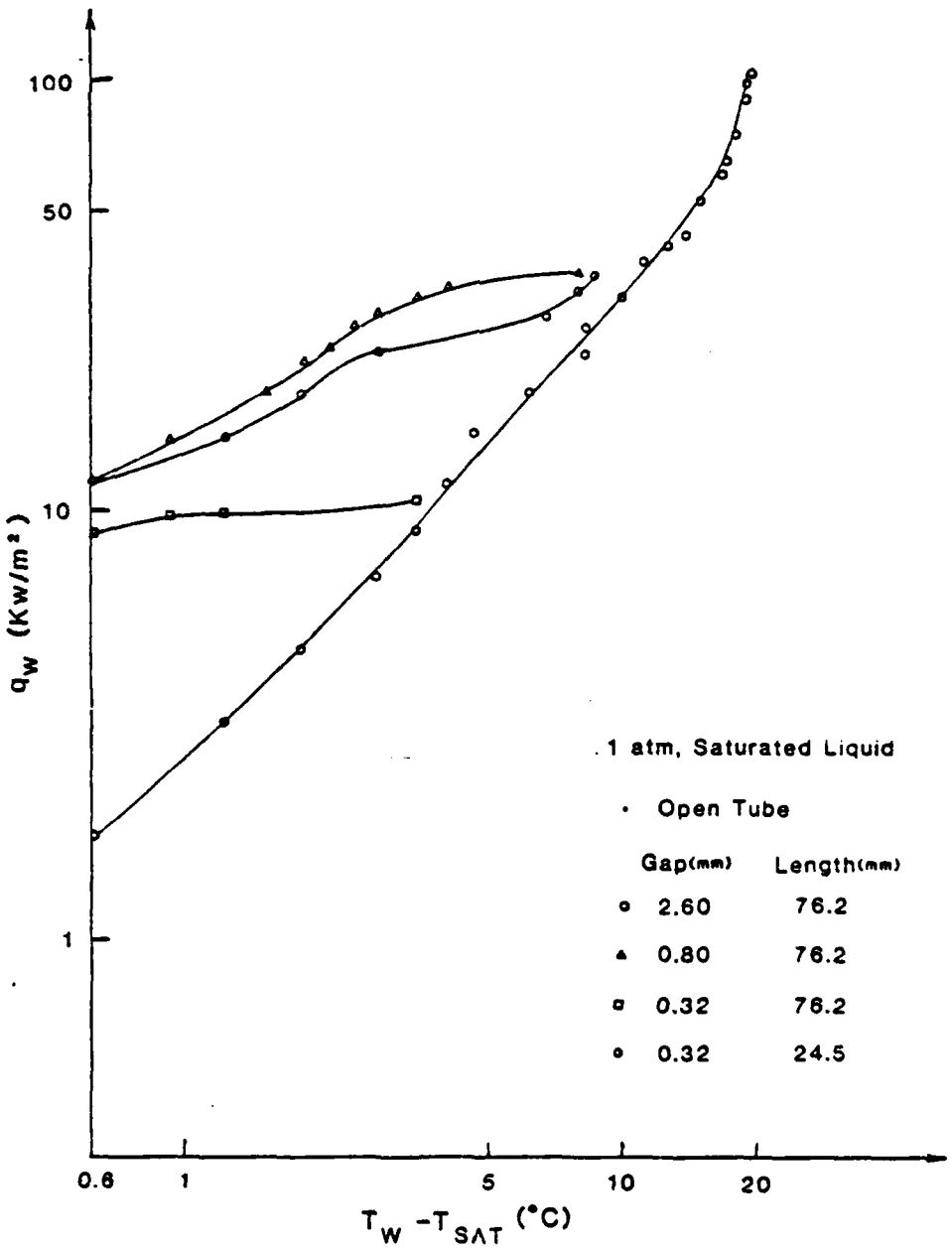

Figure 7 Boiling Curve of Acetone in the Closed Bottom Annulus

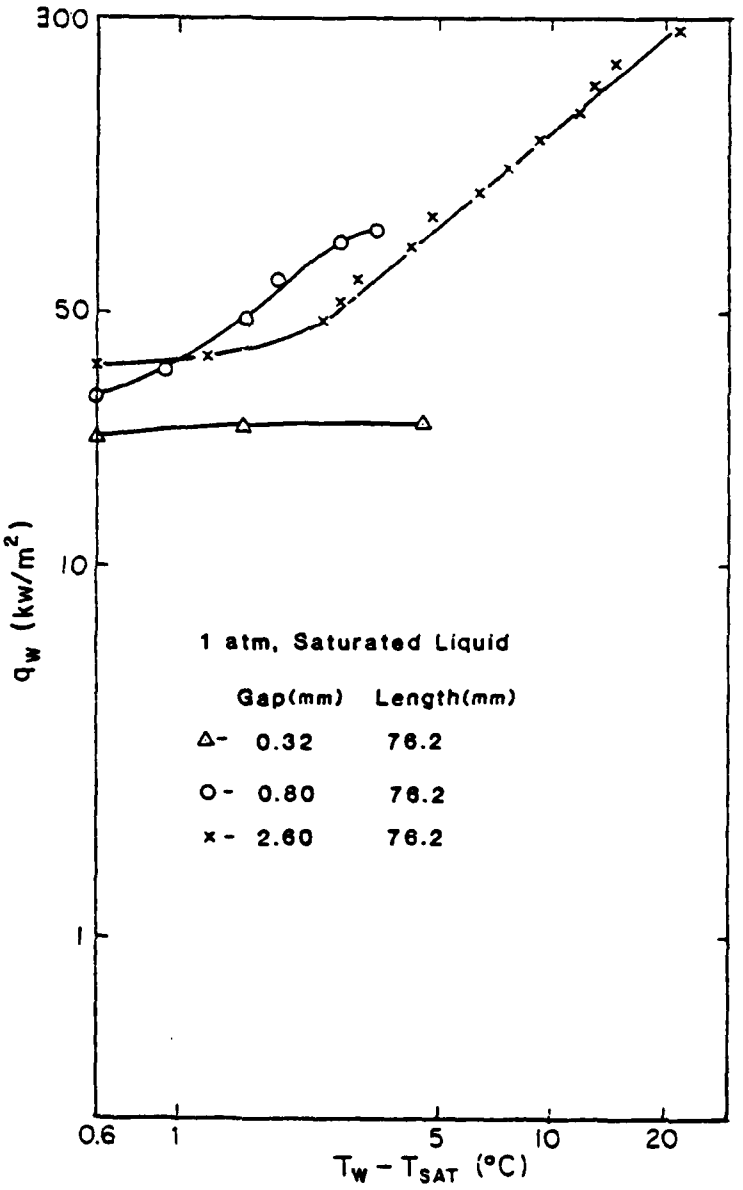

Figure 8. Boiling Curve of Water in the Closed Bottom Annulus

all the boiling curves in the present study have similar characteristic to the curves of low Bond number in Freon-113 or acetone experiments.

The relationship among the Bond number, the heat transfer characteristics, and the bubble region are shown in the following:

Table 5. The Bond No. with respect to Bubble Region and Associated Heat Transfer Characteristics

	Bond Number				
Bubble region	0.72-1.66	1.84-5.78	8.4	13.6	Infinite
Isolated Deformed Bubbles(Small Bond No. Low Heat Flux)	X	X	X		
Violent Evaporation of Deformed Bubbles (Small Bond No. High Heat Flux)		X	X	X	
Bubble Generated under Deformed Bubbles(Large Bond Number)			X	X	
Open Pool					X

From Table 5 the Bond number is a parameter to indicate the importance of boiling regions for a given system. The larger the Bond number is, the closer it is to open pool results.

3 The Dryout Heat Flux

As shown in previous sections the dryout heat flux in the crevice with the closed bottom is considerably lower than the critical heat flux for boiling in a open pool. For Freon-113 experiment, the critical heat flux of a open pool boiling is 201 kw/m^2, but for the smallest gap (0.32mm) the dryout heat flux studied presently is only 6.3 kw/m^2 , which is almost 2 order of magnitude less. The value of dryout heat flux is summarized in Table 6.

Generally, the smaller the gap size the lower the dryout heat flux. The wall super heat at dryout is also found to be decreasing with smaller gap size. The dryout heat flux decreases when the length of the crevice increases.

Table 6. The Summary of Dryout Heat Flux Data in Crevices

	S(mm)	L(mm)	P(atm)	q (kw/m^2)	T ($^\circ$ c)
Water	2.58	76.2	1	210.1	16.11
	0.80	"	"	82.0	9.72
	0.32	"	"	25.2	3.06
Acetone	2.58	76.2	"	109.5	7.78
	0.80	"	"	37.2	7.78
	0.32	25.4	"	35.0	18.33
	"	76.2	"	10.8	3.05
F-113	2.58	76.2	"	69.4	18.06
	0.80	"	"	21.1	15.83
	0.32	25.4	"	17.4	4.72
	"	76.2	"	6.29	0.83
	"	"	0.60	5.54	1.11
	"	"	2.02	7.55	0.83
	"	"	3.04	8.53	1.39
	"	"	4.04	8.78	1.67

1. Analysis

The significant difference between the pool boiling critical heat flux and the dryout heat flux of crevices may attributed to the different limiting mechanism for the liquid to come into the heating surface. Near the dryout, the outward vapor flow prohibit sufficient liquid to flow down into the crevice Fig. 9 . This phenomena is similar to that of hydrodynamic counter-current flooding in tubes. When flooding occurs the down-coming liquid becomes

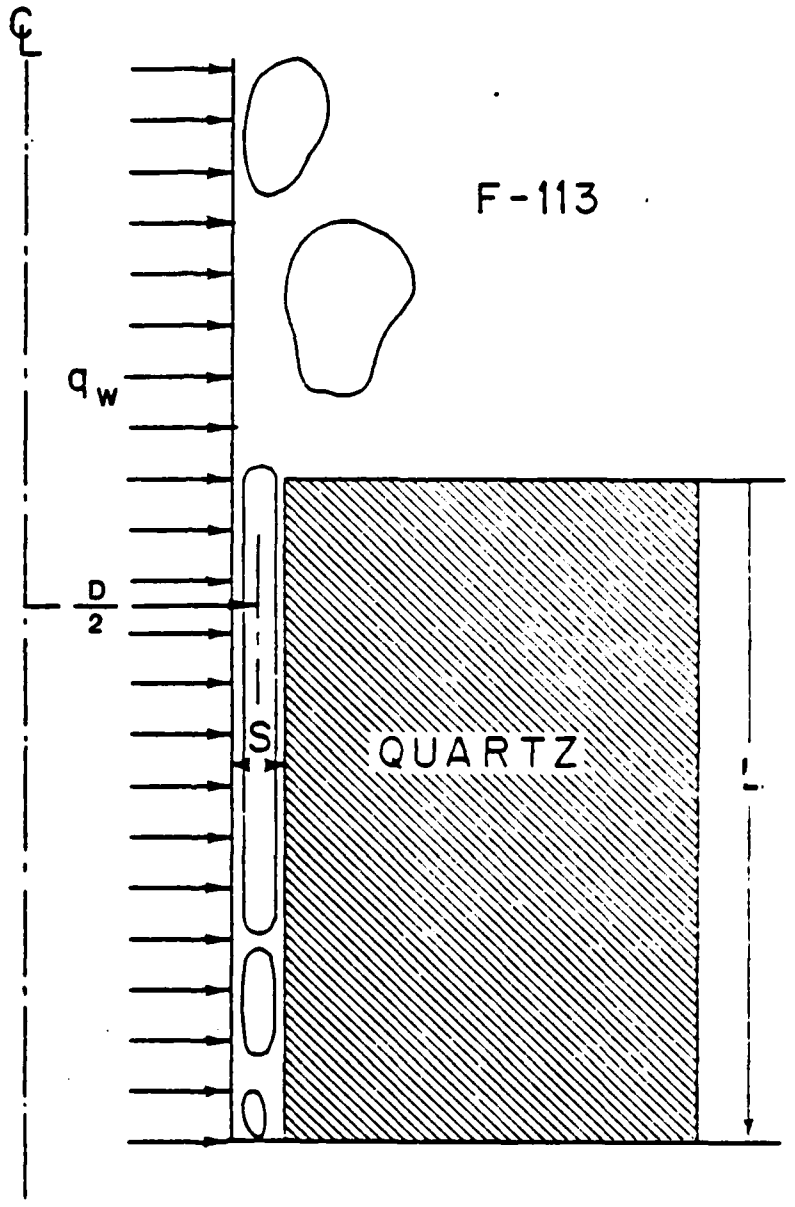

Figure 8. Fluid Behavior near Dryout Heat Flux

stagnant because the gravity force is balanced by the up going vapor shear force.

The counter-current flooding of two phase flow in a round tube is a well studied problem. For tubes with small diameter the correlation proposed by Wallis [14] base on the superficial velocities is the best fit of data. the hydrodynamic flooding experiment of the annulus geometry with Bond number equals 25 has been conducted by Shire et al [15]. The results can also be correlated satisfactorily by a similar form of Wallis correlation but with different empirical constant.

On the other hand, the dryout heat flux for tubes of different diameters has been correlated by Nejat using flooding considerations. In the derivation, Nejat [16] used the Wallis correlation together with the limiting condition for large tubes. He argued that the dryout heat flux for tubes with small diameter is a function of Bond number, and the correlated experimental data have the Bond number in the range of 18 to 100.

In the present experiment the range of Bond number for Freon-113, acetone, and distilled, demineralized water is between 0.72 and 13.6. Since the Bond number is generally small, the Wallis correlation may be used to describe the hydrodynamic counter-current flooding in crevice. For an annulus with closed bottom the flooding will start at the top opening where the vapor velocity is the highest. At a higher heat flux the dryout starts at the top of crevice. It is also important to notice that the dryout condition may occur before the flooding happens because the dryout occurs when the supply of liquid is "insufficient" to remove the heat applied to the tube. At this moment the liquid flow has not been completely stopped yet.

The Wallis correlation can be represented as

$$j_g^{*1/2} + j_f^{*1/2} = C \text{ if } Bo < 50$$

where: $j_g^* = j_g \rho_g^{1/2} \{gD(\rho_f - \rho_g)\}^{-1/2}$

$j_f^* = j_f \rho_f^{1/2} \{gD(\rho_f - \rho_g)\}^{-1/2}$

and

$j_g = M_g/(\rho_g A)$

$j_f = M_f/(\rho_f A)$

where the characteristic dimension D, which is measured from the center of the gap, is used to non-dimensionalize the superficial velocities. Since the annulus has a closed bottom, the steady state mass flow rate of liquid come in at the top opening of the crevice should equal to the mass flow rate of vapor flowing out of the top opening.

$M_g = M_f$

At the moment the dryout starts, the rate liquid flows into the crevice equal the rate liquid evaporates. The mass velocity can be related to the heat flux as

$Mg = q_w A^*/H_{fg}$

By substituting and rearranging the equations and assuming the gap size is much smaller than the diameter, the dryout heat flux can be represented as

$B_l x(1+(\rho_f/\rho_g)^{1/4})^2 x \rho_g/\rho_f = 2C^2$

where $B_l = q_w L/H_{fg} \rho_g VS$

and $V = \rho_f^{-1/2}(gD(\rho_f-\rho_g))^{1/2}$

The boiling number Bo is defined as a ratio of outgoing vapor velocity ($q_w L/H_{fg}\rho_g S$) to the bubble rising velocity($\rho_f^{-1/2}(gD(\rho_f-\rho_g))^{1/2}$) in the annulus [14] . The characteristic dimension for the annulus is the diameter of the annulus D which is measured at the middle of the gap. In terms of the diameter of the inner tube D and the gap thickness S the D is

$$D = Di + S$$

The dryout heat flux of present study for Freon-113, acetone and distilled demineralized water in crevices of different gaps and heights can be correlated by the above formulation. In addition, the water experimental data of Kusuda & Imura [8] with Bond number 3.17-18 is also correlated. The results are shown in Figure 10.

All these data can be correlated properly in the form of

$$B_i x(1+(\rho_f/\rho_g)^{1/4})^2 x \rho_g/\rho_f = 0.38$$

It is important to include the results of Kusuda & Imura into the correlation. In their experiment the annulus is heated from outside wall. However, the present experiments are heated from inside tube. The dryout heat flux correlation is independent of the side which is heated.

The crevice of the smallest size (0.32mm) has also been tested in Freon-113 pool at different pressures. In general, the behavior of boiling at other pressures is similar to that discussed previously. At elevated pressure the bubbles appear to be slightly more toward spherical shape. The dryout heat flux is also fitted well by the proposed correlation.

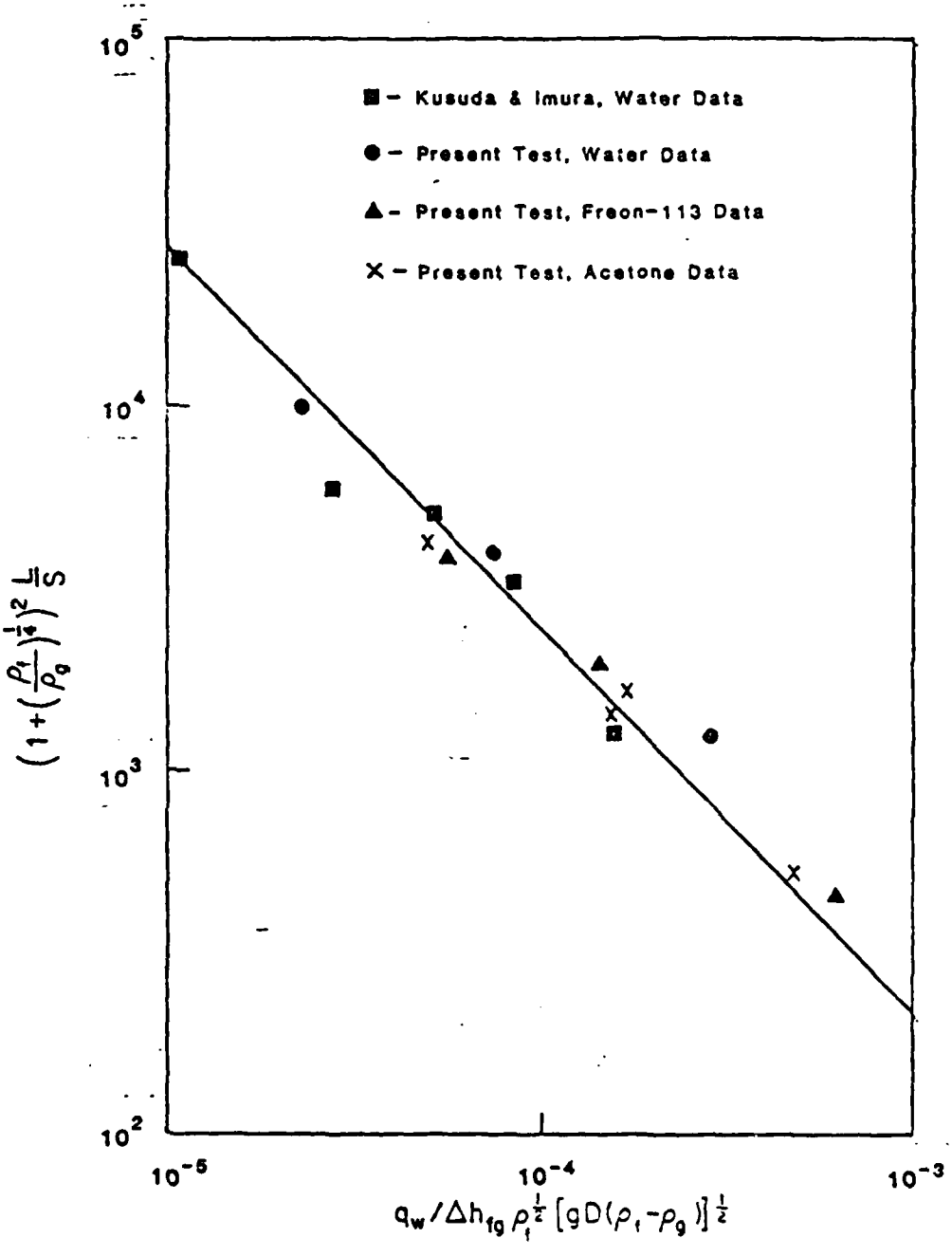

Figure 10. Dryout Correlation for closed Bottom vertical Annulus

It is generally observed that the Wallis hydrodynamic flooding correlation for small gaps is independent of the surface tension. Therefore, the present dryout heat flux correlation is, similarly, independent of the surface tension. Although the water has 3 times larger surface tension than that of Freon-113 and acetone these data can be correlated satisfactorily by the equation which does not containing the surface tension.

CONCLUSIONS AND RECOMMENDATIONS

1 Conclusions

1. From the visual observation the boiling in the confined space has three different boiling regions: isolated deformed bubble, violent evaporation of deformed bubble and bubble nucleated on the solid surface. Bond number can be used as a parameter to indicate the existence of boiling regions for a giving system.

2. For the small Bond number and low heat flux, the heat flux increases with little increase of wall temperature. The boiling is characterized as many isolated deformed bubbles. At higher heat flux, the wall temperature increases proportional to heat flux and the boiling is under violent evaporation of deformed bubble. For large Bond number, heat flux can go even higher with small bubbles with bubble nucleated on the solid surface. The heat transfer characteristic is similar to pool boiling curve but with slight less wall superheat. The Larger the Bond number is, The closer the results to pool boiling curve.

3. The heat transfer under the isolated deformed bubble is dominated by thin film evaporation. The increasing of heat flux increases the area covered by deformed bubbles,but not changing the wall superheat temperature.

4. Under the condition of having bubbles nucleated on solid surface, the reduction of wall superheat comparing to open pool boiling curve is attributed to the convective effect.

5. The dryout heat flux in the confined space is much lower than that in the pool boiling. The correlation for dryout heat flux, derived from the counter-current flooding condition, fit the experimental data within ±24 % for various liquids at different conditions. For annulus heated from inside tube or outside wall the dryout heat flux can be correlated with the same correlation proposed here.

2 Recommendations for Further Study

1. Boiling with isolated deformed bubble shows very good heat transfer characteristics. The further study on this phenomena may result in better understanding of heat transfer augmentation in confined space.

2. For the purpose of understanding the thermohydraulic induced corrosion in the heat exchanger of PWR, the dryout heat flux for eccentric annulus should be studied. It is the likely case in the real heat exchangers.

3. The dryout heat flux of confined space with both ends is suspected to be a phenomenon of counter-current flooding also. For open ends the liquid may enter the confined space form the bottom end. The conservation of mass used in our analysis of closed bottom annulus may not be applied directly. With some modification in the derivation of equations and carefully perform experiments similar type of dryout correlation may be obtained.

4. The heat exchanger in the nuclear submarine is placed horizontally. The same corrosion problem may occur. It is valuable to study the horizontal closed bottom annulus. It is suspected that the boiling behavior of isolated deformed bubble remains the same.

6. This test was done with an active nucleation site at the bottom, it will be interesting to study the boiling in the confined space without such a site exists.

REFERENCES:

1. Katto, Y., Yokoya, S.
Experimental Study of Nucleate Pool Boiling in Case of Making Interference-Plate Approach to the Heating Surface.
In *Third Intl. Heat Transfer Conf.*, pages 219-227. 1966.

2. Katto, Y., Yokoya,S.
Principle Mechanism of Boiling Crisis in Pool Boiling.
Intl. J. Heat Mass Transfer 2:993, 1968.

3. Katto, Y., Yokoya, S., Ysunaka, M.
Mechanism of boiling Crsis and Transition Boiling in pool Boiling.
In *Fourth Intl. Heat Transfer Conf.*, pages 332. 1970.

4. Katto, Y., Yokoya, S., Teraoka, K.
Nucleate and Transition Boiling in a Narrow Space between Two Horizontal, Parallel Disk Surfaces.
Bulletin of JSME 20(143), 1977.

5. Ishibashi, E., Nishkawa, K.
Saturated Boiling Heat Transfer in Narrow Space.
Intl. J. Heat Mass Transfer 12:863-894, 1969.

6. Jensen M. K., Cooper P. E., Bergles A. E.
Boiling Heat Transfer and Dryout in Restricted Annular Geometries.
In *16th National Heat Transfer Conference*, pages 205-214. AICHE, 1976.
Paper No. AICHE-14.

7. Kusuda, H., Imura, H.
Boiling Heat Transfer in an Open Thermosyphon.
Bulletin of JSME 16(101):1723-1740, Nov., 1973.
Report 1 & 2.

8. Kusuda, H., Imura, H.
Stability of a Liquid Film in a Counter-Current Annular Two-Phase Flow.
Bulletin of the JSME 17(114):1613-1618, Dec., 1974.

9. Eckert, E.
Introduction to the Transfer of Heat and Mass.
McGraw-Hill Book Company, Inc., New York, 1951.

10. Yilmaz, S. Westwater, J. W.
Effect of Velocity on Heat Transfer to Boiling F-113.
J. of Heat Transfer 102:26-31, Feb., 1980.

11. Hesse, G.
Heat Transfer in Nucleate Boiling, Maximum Heat Flux and Transition Boiling.
Intl. Heat and Mass Transfer 16(8):1611-1627, 1973.

12. Chernobyl'skii, I. I. and Tananiko, Iu. M.
Heat Exchange during Boiling of Liquids in Narrow Annular Tubes.
Soviet Phys. :1244-1249, 1966.
Technical Physics.

13. Griffith, P. and Wallis, J. D.
The Role of Surface Condition in Nucleate Boiling.
In *Chem. Eng. Prog. Symp.*, pages 49-63. 1960.
Ser. 56.

14. Wallis, G. B.
One-dimensional Two-phase Flow.
McGraw-Hill Book Company, Inc., 1969.

15. Shire, G. L. ,Pickering, A. R.,and Blacker, P. T.
Film Cooling of Vertical Feul Rods.
Technical Report AEEW-R343, UKAEA, 1964.

16. Nejat, Z.
Maximum Heat Flux for Countercurrent Two Phase Flow in a Closed End Vertical Tube.
In *Sixth Intl. Heat Transfer Conf.*, pages 441-444. 1978.

AD-A107 363 CARNEGIE-MELLON UNIV PITTSBURGH PA DEPT OF MECHANICA--ETC F/G 20/13
BOILING HEAT TRANSFER IN CONFINED SPACE.(U)
OCT 81 S YAO
N00014-79-C-0623
UNCLASSIFIED
NL

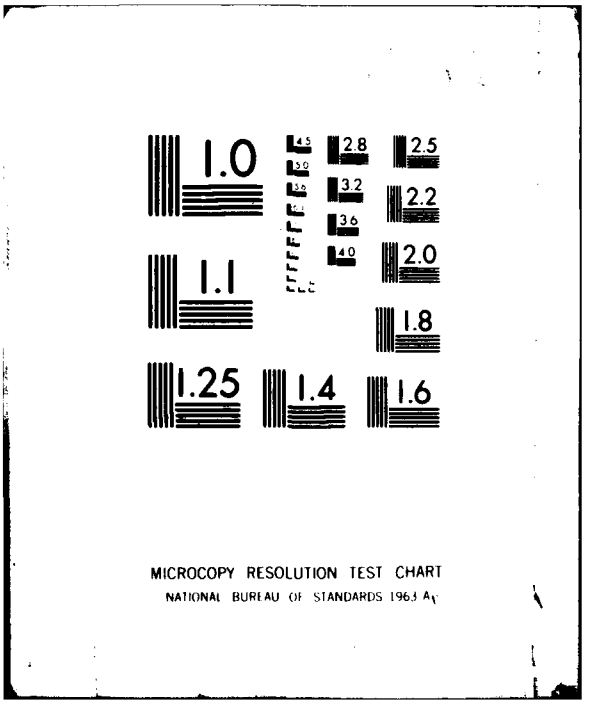
1.0
1.1
1.25
1.4
1.6
1.8
2.0
2.2
2.5
2.8
3.2
3.6
4.0
MICROCOPY RESOLUTION TEST CHART
NATIONAL BUREAU OF STANDARDS 1963 A

CHAPTER 5

EXPERIMENTS OF CONVECTIVE BOILING AND DRYOUT IN ANNULAR CREVICES

Boiling of dryout in annular crevices with forced convective is under study currently. The loop has been constructed. The schematic of the loop is shown in Fig. 1 with the loop characteristics summarized in it. In order to perform boiling experiments at constant pressures, an accumulator is attached to the loop to absorb the volume expansion of the two phase fluid duirng the tests. Large flow by-pass is provided to the test section to maintain the flow stability in the test section. The instrumentation system has also been established.

The schematic of the test section is shown in Fig. 2. The quartz test section is changeable for different lengths and annular gaps.

The data of the smallest gap annulus are shown in Fig. 3. The general feature is similar to that of conventional boiling curve of large-gap annulus but with relatively low wall superheat and low critical heat flux. The trend of the critical heat flux with respect to the mass flux also similar to the conventional boiling however with lower values of critical heat flux.

Other data are undertaking and more detailed results and discussion will be available soon.

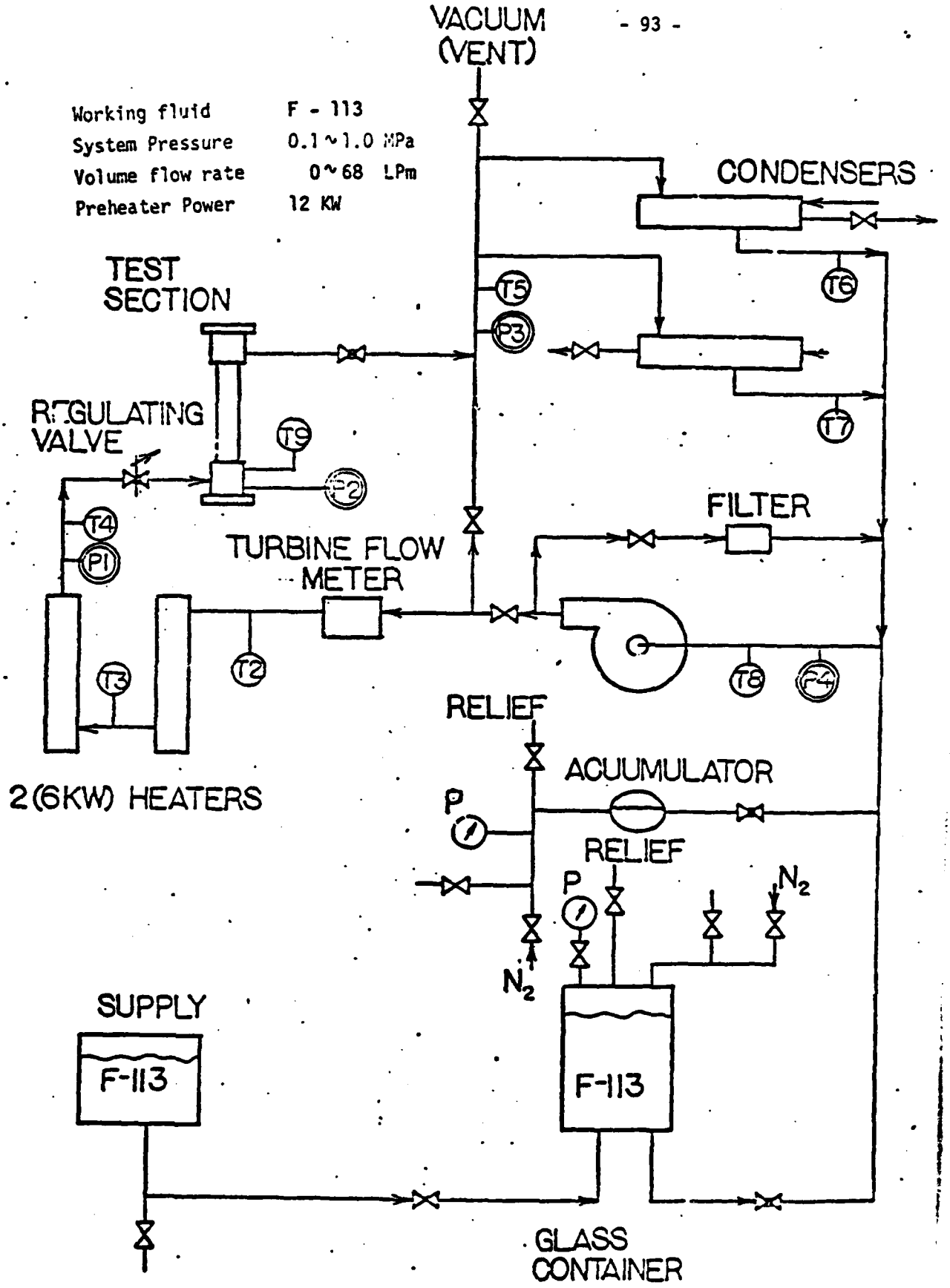
VACUUM
(VENT)
Working fluid F - 113
System Pressure 0.1 ~ 1.0 MPa
Volume flow rate 0 ~ 68 LPm
Preheater Power 12 KW
CONDENSERS
TEST
SECTION
T5
P3
T6
T7
REGULATING
VALVE
T9
P2
FILTER
T4
P1
TURBINE FLOW
METER
T2
T3
T8
P4
RELIEF
ACUUMULATOR
2(6KW) HEATERS
P
RELIEF
P
N2
N2
SUPPLY
F-113
F-113
GLASS
CONTAINER

Figure 1

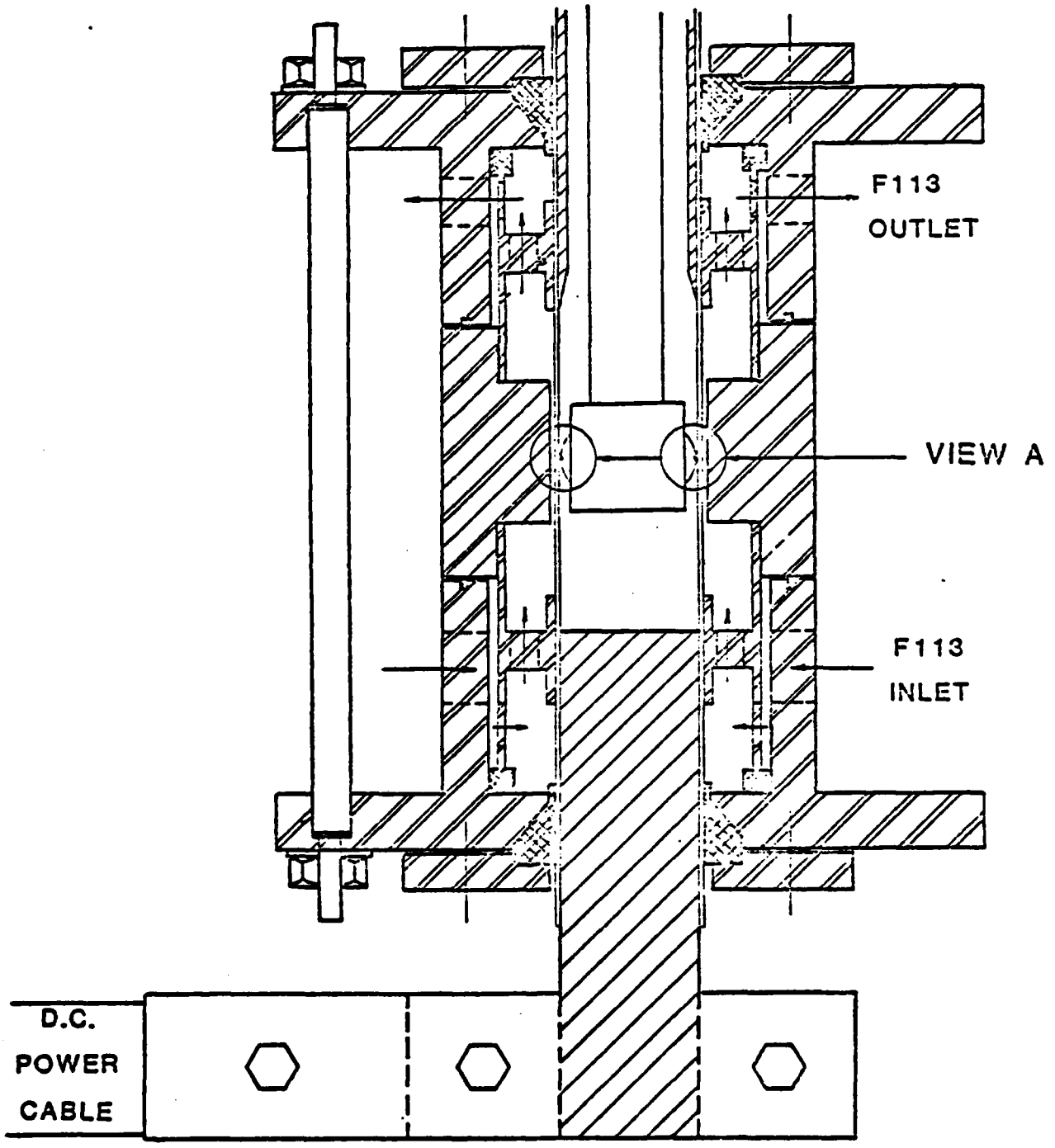

Fig. 2.

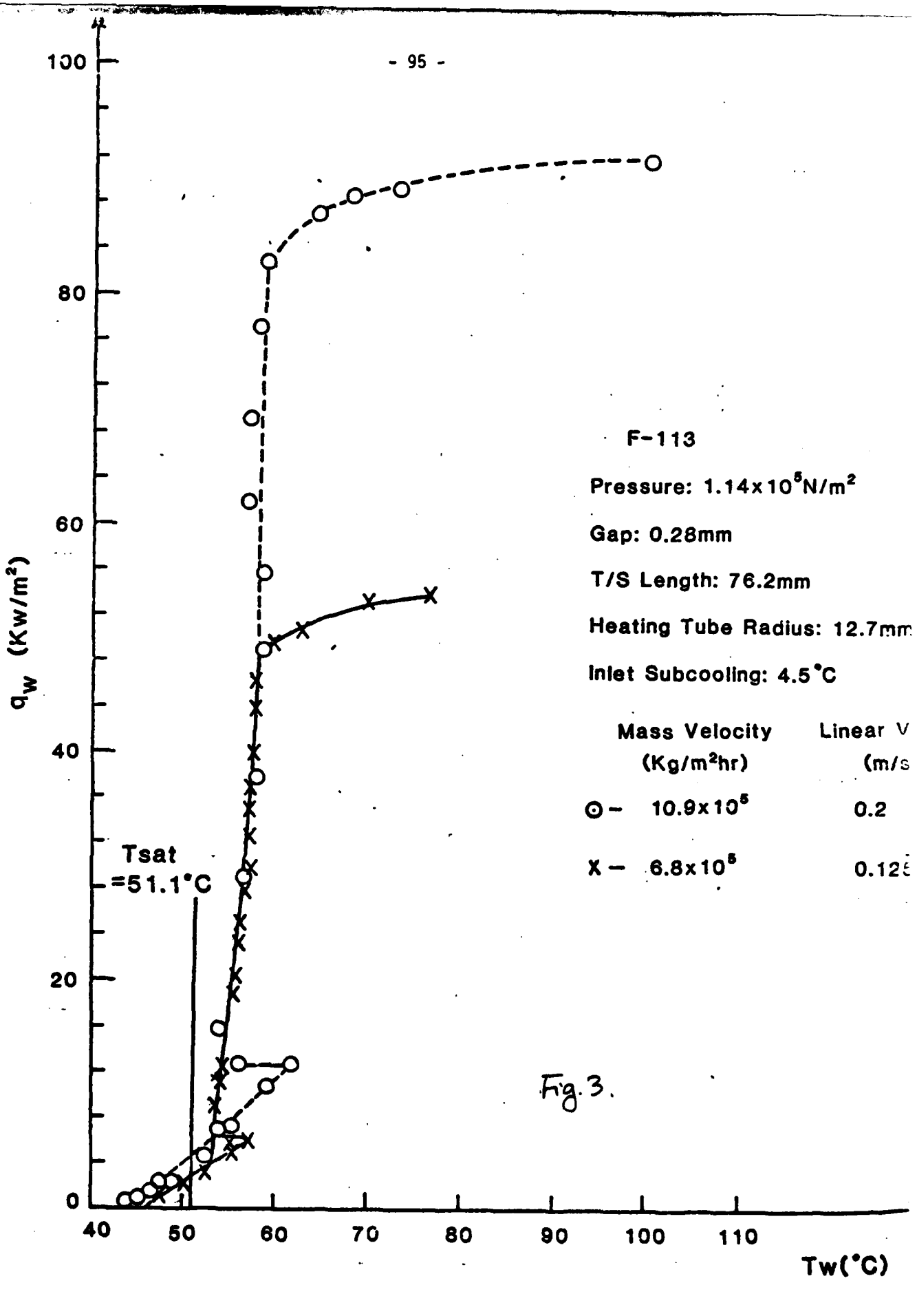
100
80
60
40
20
0
q_w (Kw/m²)
Tsat
=51.1°C
40
50
60
70
80
90
100
110
Tw(°C)
F-113
Pressure: 1.14x10⁵N/m²
Gap: 0.28mm
T/S Length: 76.2mm
Heating Tube Radius: 12.7mm
Inlet Subcooling: 4.5°C
Mass Velocity (Kg/m²hr)
Linear V (m/s
⊙ – 10.9x10⁵ 0.2
X – 6.8x10⁵ 0.12

Fig. 3.

DISTRIBUTION LIST

HEAT TRANSFER

	One copy except as noted
Mr. M. Keith Ellingsworth Power Program Office of Naval Research 800 N. Quincy Street Arlington, VA 22217	5
Defense Documentation Center Building 5, Cameron Station Alexandria, VA 22314	12
Technical Information Division Naval Research Laboratory 4555 Overlook Avenue SW Washington, DC 20375	6
Professor Paul Marto Department of Mechanical Engineering US Naval Post Graduate School Monterey, CA 93940	
Professor Bruce Rankin Naval Systems Engineering US Naval Academy Annapolis, MD 21402	
Office of Naval Research Eastern/ Central Regional Office Bldg 114, Section D 666 Summer Street Boston, Massachusetts 02210	
Office of Naval Research Branch Office 536 South Clark Street Chicago, Ill. 60605	
Office of Naval Research Western Regional Office 1030 East Green Street Pasadena, CA 91106	
Mr. Charles Miller, Code 05R13 Crystal Plaza #6 Naval Sea Systems Command Washinton, DC 20362	

Steam Generators Branch, Code 5222
National Center #4
Naval Sea Systems Command
Washington, DC 20362

Heat Exchanger Branch, Code 5223
National Center #3
Naval Sea Systems Command
Washington, DC 20362

Mr. Ed Ruggiero, NAVSEA 08
National Center #2
Washington, DC 20362

Dr. Earl Quandt Jr., Code 272
David Taylor Ship R&D Center
Annapolis, MD 21402

Mr. Wayne Adamson, Code 2722
David Taylor Ship R&D Center
Annapolis, MD 21402

Dr. Win Aung
Heat Transfer Program
National Science Foundation
Washington, DC 20550

Mr. Michael Perlsweig
Department of Energy
Mail Station E-178
Washington, DC 20545

Dr. W.H. Theilbahr
Chief, Energy Conservation Branch
Dept. of Energy, Idaho Operations Office
550 Second Street
Idaho Falls, Idaho 83401

Professor Ephriam M. Sparrow
Department of Mechanical Engineering
University of Minnesota
Minneapolis, Minnesota 55455

Professor J.A.C. Humphrey
Department of Mechanical Engineering
University of California, Berkeley
Berkeley, California 94720

Professor Brian Launder
Thermodynamics and Fluid Mechanics Division
University of Manchester
Institute of Science & Technology
P088 Sackville Street
Manchester M601QD England

Professor Shi-Chune Yao
Department of Mechanical Engineering
Carnegie-Mellon University
Pittsburgh, PA 15213

Professor Charles B. Watkins
Chairman, Mechanical Engineering Department
Howard University
Washington, DC 20059

Professor Adrian Bejan
Department of Mechanical Engineering
University of Colorado
Boulder, Colorado 80309

Professor Donald M. McEligot
Department of Aerospace and Mechanical Engineering
Engineering Experiment Station
University of Arizona 85721

Professor Paul A. Libby
Department of Applied Mechanics and Engineering Sciences
University of California San Diego
Post Office Box 109
La Jolla, CA 92037

Professor C. Forbes Dewey Jr.
Fluid Mechanics Laboratory
Massachusetts Institute of Technology
Cambridge, Massachusetts 02139

Professor William G. Characklis
Dept. of Civil Engineering and Engineering Mechanics
Montana State University
Bozeman, Montana 59717

Professor Ralph Webb
Department of Mechanical Engineering
Pennsylvania State University
208 Mechanical Engineering Bldg.
University Park, PA 16802

Professor Warren Rohsenow
Mechanical Engineering Department
Massachusetts Institute of Technology
77 Massachusetts Avenue
Cambridge, Massachusetts 02139

Professor A. Louis London
Mechanical Engineering Department
Bldg. 500, Room 501B
Stanford University
Stanford, CA 94305

Professor James G. Knudsen
Associate Dean, School of Engineering
Oregon State University
219 Covell Hall
Corvallis, Oregon 97331

Professor Arthur E. Bergles
Mechanical Engineering Department
Iowa State University
Ames, Iowa 50011

Professor Kenneth J. Bell
School of Chemical Engineering
Oklahoma State University
Stillwater, Oklahoma 74074

Dr. James Lorenz
Component Technology Division
Argonne National Laboratory
9700 South Cass Avenue
Argonne, Illinois 60439

Dr. David M. Eissenberg
Oak Ridge National Laboratory
P.O. Box Y, Bldg. 9204-1, MS-0
Oak Ridge, Tennessee 37830

Dr. Jerry Taborek
Technical Director
Heat Transfer Research Institute
1000 South Fremont Avenue
Alhambra, CA 91802

Dr. Simion Kuo
Chief, Energy Systems
Energy Research Laboratory
United Technology Research Center
East Hartford, Connecticut 06108

Mr. Jack Yampolsky
General Atomic Company
P.O. Box 81608
San Diego, CA 92138

Mr. Ted Carnavos
Noranda Metal Industries, Inc.
Prospect Drive
Newtown, Connecticut 06470

Dr. Ramesh K. Shah
Harrison Radiator Division
General Motors Corporation
Lockport, New York 14094

Dr. Ravi K. Sakhuja
Manager, Advanced Programs
Thermo Electron Corporation
101 First Avenue
Waltham, Massachusetts 02154

Mr. Robert W. Perkins
Turbotec Products, Inc.
533 Downey Drive
New Britain, Connecticut 06051

Dr. Keith E. Starner
York Division, Borg-Warner Corp.
P.O. Box 1592
York, PA 17405

Mr. Peter Wishart
C-E Power Systems
Combustion Engineering, Inc.
Windsor, Connecticut 06095

Mr. Henry W. Braum
Manager, Condenser Engineering Department
Delaval
Front Street
Florence, New Jersey 08518

Dr. Thomas Rabas
Steam Turbine-Generator Technical Operations Division
Westinghouse Electric Corporation
Lester Branch
P.O. Box 9175 N2
Philadelphia, PA 19113

Professor Daryl Metzger
Chairman, Mechanical and Energy
Systems Engineering
Arizona State University
Tempe, Arizona 85281

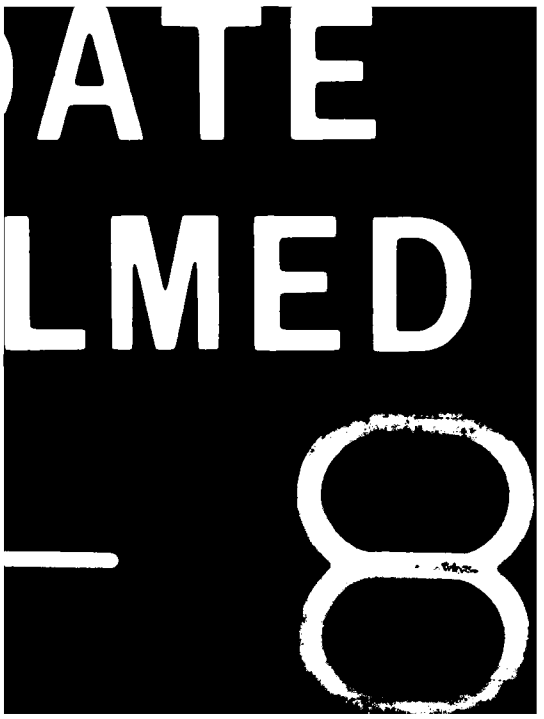
ATE
LMED
8